Delft University of Technology

Bachelor thesis

Bachelor Applied Physics & Applied Mathematics

Eclipses by exomoons

Author:
Maaike A. Mol
4395913

Supervisors:
Dr. Paul M. Visser
Dr. Aurèle J. L. Adam
Dr. Wolter G. M. Groenevelt
Dr. Akira Endo

Delft University of Technology,

Faculty of Applied Sciences &
Faculty of Electrical Engineering, Mathematics and Computer Science,

August 23, 2018

Abstract

The aim of this research is to study a method to find exomoons and to find specific characteristics that point to the existence of exomoons. Exomoons are natural satellites orbiting an extrasolar (exo)planet in an extrasolar system. By looking at eclipses on exoplanets, we can find these characteristics.
We consider the reflected light signals of exoplanets with an exomoon. The reflected light signal is the intensity of light the planet reflects from the host star towards the observer.
We derive the reflected light signal in a planetary system with one exoplanet and in a system with an exoplanet and an exomoon. We made the assumptions that the exoplanets and exomoons have a homogeneous surface (albedo is 1) and move in circular orbits around a star with an inclination angle between the orbital planes. Along the orbit the planet and the moon have changing phases. The moon is always close to its planet, so the phases of the exomoon and the exoplanet are the same. For exoplanets, it is not possible to spatially separate a moon from its planet. One only sees the total signal of both bodies, the light originating from the star, reflected by the two bodies towards the observer.
Maybe we can find an exomoon by examining eclipses. Eclipses occur when the exoplanet and exomoon are aligned with the star, so that the body closest to the star blocks the light towards the body farthest from the star. Finding eclipses is one of the few methods to discover exomoons. The systems are modeled with the assumption that any total eclipse happens every time $\hat{r} = \hat{R}$ or $-\hat{r} = \hat{R}$, we see short dips in the reflected light signal. These dips are periodic and make the complete signal quasi-periodic. That is why we also calculate the Fourier transform of the reflected light signal. This quasi-periodicity causes the Fourier spectrum to have side bands that are repeated and are copies of themselves.
In this research, the orbit of the exomoon is tilted to see the effect of inclination in the reflected light signal. The result is fewer eclipses. At most twice a year for a short amount of time an eclipse can occur. In the Fourier domain, this results in more peaks, but the pattern is still repeated.
From this research, we cannot conclude whether or not an exomoon is present from measured data. What we learned, is that if an exomoon is present, short dips in the received light signal occur and this results in periodic side bands in the Fourier domain with respect to the system of one planet. The duration of an eclipse is very short, so the detection of the eclipse can easily be missed. The Fourier transform signal becomes stronger when a longer time has been measured.

Contents

Nomenclature

Symbol	Unit	Value	Description
t	[s]		Time
t_n	[s]		Time the nth eclipse occurs
$\tilde{t}_n$	[s]		Time the nth eclipse occurs on the planet
$\hat{t}_n$	[s]		Time the nth eclipse occurs on the moon
R_{Jup}	[m]	$69911 \cdot 10^3$	Jupiter radius
S	[m]	10^9	Radius of the star
s	[Radius Jupiter]	1	Radius of the exoplanet
s_1	[Radius Jupiter]		Radius of the planet
s_2	[Radius Jupiter]		Radius of the moon
ρ_{Jup}	[kg m^{-3}]	$1.33 \cdot 10^3$	Density of Jupiter
V_1	[m^3]	$\frac{4}{3}\pi s_1^2$	Volume of the planet
V_2	[m^3]	$\frac{4}{3}\pi s_2^2$	Volume of the moon
M	[Solar Mass kg]	3	Mass of the star
m_1	[Jupiter Mass kg]	$\rho_{Jup} \cdot V_1$	Mass of the planet
m_2	[Jupiter Mass kg]	$\rho_{Jup} \cdot V_2$	Mass of the moon
ω	[rad]	$\frac{2\pi}{73 \cdot 24 \cdot 3600}$	Angular frequency of binary orbit
Ω	[rad]	$\frac{2\pi}{5 \cdot 24 \cdot 3600} + \omega$	Angular frequency of the planet-moon orbiting their barycenter
α	[°]		Tilt in plane of the planet and the moon
α^*	[-]		Inclination value
G	[m^3 s^{-2} kg^{-1}]	$6.674 \cdot 10^{-11}$	Gravitation constant
P_0	[W]		The power of the star
P_{ob}	[W]		Power observed by the observer
P_s	[W]		Power observed by the planet
R	[m]	$\left(\frac{GM}{\omega^2}\right)^{\frac{1}{3}}$	Distance from the star to the center of mass of the planet and the moon
$\vec{R}(t)$	[m]		Position vector of the center of mass of the planet and the moon
$\vec{R}_1(t)$	[m]		Position vector of the planet
$\vec{R}_2(t)$	[m]		Position vector of the moon
$\hat{R}(t)$	[]		Normalized $\vec{R}(t)$
$\hat{R}_1(t)$	[]		Normalized $\vec{R}_1(t)$
$\hat{R}_2(t)$	[]		Normalized $\vec{R}_2(t)$
r	[m]	$\left(\frac{G(m_1+m_2)}{\Omega^2}\right)^{\frac{1}{3}}$	Distance between the planet and the moon
$\vec{r}(t)$	[m]		Reduced vector from the planet to the moon
$\hat{r}(t)$	[]		Normalized reduced vector
x, y and z	[m]		Cartesian coordinate system
μ	[rad]		Azimuthal angle on the planet or the moon surface
ν	[rad]		Polar angle to the z-axis in the planet or the moon surface
θ	[rad]	ωt	Angle between $\vec{R}$ and the x-axis in the $z = 0$ plane

ϕ	[rad]	Ωt	Angle between $\vec{r}$ and the x-axis in the $z = 0$ plane
$\vec{s}(\mu, \nu)$	[m]		Vector from the center of the planet/moon to a surface point on the planet/moon
$\hat{s}(\mu, \nu)$	[]		Normalized vector of $\vec{s}(\mu, \nu)$
$\hat{o}$	[]	$\hat{x}$, $\hat{y}$ or $\hat{z}$	The normalized vector from the system towards the observer
$\mathcal{D}$	[-]		Domain on the surface that is illuminated and visible
$d^2\Omega_{ob}$	[-]		Solid angle to the observer
$d^2\Omega_s$	[-]		Solid angle to the planet or moon
$d\vec{S}$	[m^2]		Surface vector
$M(\hat{s}, t)$	[-]	1	Mapping function
N_μ	[-]	100	Number of values in μ
N_ν	[-]	100	Number of values in ν
$\vec{P}$	[m]		Point on the surface of the planet
$\vec{P}'$	[m]		$\vec{P}$ projected on $\vec{R}(t)$
$f(t)$	[-]		Reflected light signal
$f_1(t)$	[-]		Reflected light signal of the planet
$f_2(t)$	[-]		Reflected light signal of the moon
$f_B(t)$	[-]		Reflected light signal of the planet and the moon
$\hat{f}(\nu)$	[-]		Fourier transform of the reflected light signal
$f_D(t)$	[-]		Part of the reflected light signal due to phases
$f_E(t)$	[-]		Part of the reflected light signal due to eclipses
$\mathcal{A}$	[-]		Rotational matrix
h	[m]		Heigth of the eclipse cone
l	[m]		Displacement in the motion of the moon with respect to the planet
l_{max}	[m]		Maximum value of l

1 Introduction

Extrasolar planets or exoplanets are planets that orbit a different star in space than the Sun. Exoplanets are extremely difficult to discover, due to their small radius compared to their host star. Often new exoplanets are discovered. Currently, there are already 3735 confirmed exoplanets by various detection methods [1]. Scientists are mainly searching for Earth-like planets, planets that are in the habitable zone of its star and that could contain life forms. Because more exoplanets are discovered everyday, the number of opportunities to find life in the universe is constantly increasing.
An exomoon is a natural satellite of an exoplanet [2]. Some scientists think extrasolar moons, or simply, exomoons, are good candidates for life elsewhere in the universe [2]. The Kepler mission found hundred of exoplanets which could have a moon, including 70 where the radius of the exomoon is expected to be larger than the Earth radius [3]. But up until now, no exomoon has been discovered yet [4].
Some methods currently used to find exoplanets are: the transit method, radial velocity, microlensing and direct imaging. Direct imaging is conceptually simple, but it is very difficult to achieve. The transit method detects exoplanets by measuring a small dip in the light signal of a star as an orbiting planet passes between it and the Earth [5]. The transit method is by far the most effective detection method. Microlensing is an effect where two stars are aligned with the Earth. The star the farthest from the Earth looks bigger by the bending of light rays by the gravity of the other star. If an exoplanet orbits the closest star, the exoplanet bends the rays more intensely. From Earth it temporary looks as if the farthest star is enormous. We see a temporary peak of brightness in the light signal. The radial velocity method measures the perturbation in the movement of a star by gravitational pull of a planet in orbit [6]. This method uses Doppler spectroscopy to display changes in the movement.
Proposed methods to detect exomoons are direct imaging, microlensing, transit timing effects and the transit method. The transit timing effects have been exploited in research as in [7]. The transit method is elaborated on in for example [8], [9] and [10].
In this thesis we study a different and not very common detection method using direct light. Sometimes, if the planet is very large and the distance to the star is big, the planet can be imaged. An exomoon, however, cannot be resolved from an exoplanet by our telescopes, only the total light signal can be measured. Therefore we look at the total reflected light signal by all the bodies around the star. The reflected light signal has been studied for a system with one exoplanet in [11]. We calculate the total light signal reflected by planet and its moon. For small planets the starlight is too bright. In that case we block the direct light from the star with an coronagraph to see the weak reflection of the planet.
We think eclipses and occultations are important for the discovery of exomoons. Eclipses occur when the exoplanet and exomoon are aligned with the star. The body farthest from the star lies in the shadow of the other for a short moment. The phase of the exoplanet and exomoon are the same, so the reflected light for the planet and the moon give the same phase-dependent signal. Maybe we use the effect of eclipses to find a moon. This is the reason why we calculate eclipses to find exomoons. An occultation is an occurrence where the exoplanet, exomoon and Earth are aligned. A body blocks the reflected light from the other body to the Earth. Eclipses and occultations occur with some periodicity, which will cause in dips in the reflected light signal. Furthermore, we compute the Fourier spectra of the light signals to make the periodicity visible in peaks in the Fourier transform of the signal.

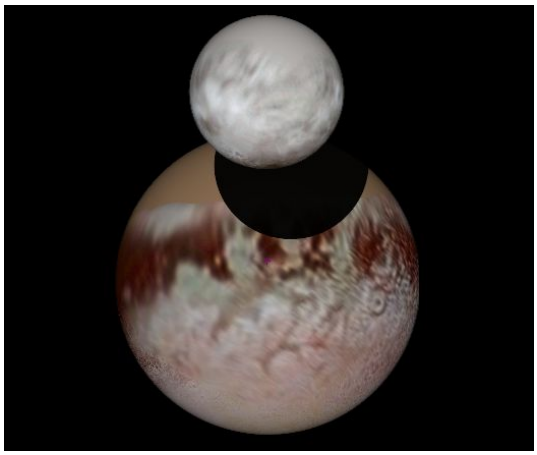

Figure 1.1: *An simulated image of an eclipse on Pluto, created by its moon Charon [12].*

In this research the aim is to model an extra-solar system with an exoplanet with exomoon and find characteristics in the light signals and Fourier spectra due to eclipses. In section 2 we will study the reflected light signal of a system with a star and one exoplanet from Earth. In section 3 we will study the reflected light signal of a system with a star and binary-planet. The change due to a moon will be elaborated on. In section 4 the Fourier spectra of the light signals of the systems are displayed and studied. In section 5, a slight inclination is taken into account in the system and the effect on the reflected light signal is studied. The observer's view is also changed. Finally in section 6, we conclude with characteristics of the reflected light signal for a planet-binary system.

2 One planet

To know what the reflected light signal is, we will start with a description of a model with one planet. In this section the reflected light signal of this system is derived, as well as the variations it undergoes by different phases of the planet.

2.1 Model and assumptions

First we will look at a extra-solar system with a star with radius S in the origin and one planet with radius s orbiting the star. The motion of a planet around a star lies in a plane [13]. We choose the planet in a circular orbit traveling in the xy-plane at a distance R from the star. An observer in the positive $\hat{x}$-direction is observing this system from far away, see figure 2.1.

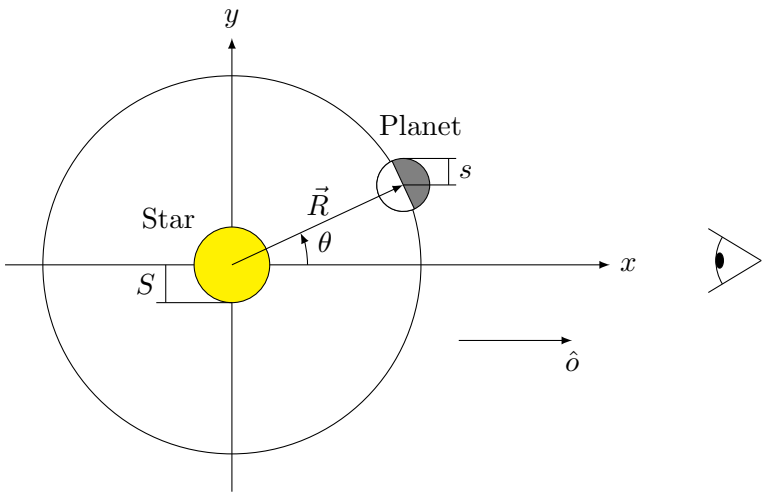

Figure 2.1: *A figure of the system. The figure is depicted face-on (top view). The star with radius S is located in the origin. The planet with radius s orbits around the star in a circular orbit in the xy-plane with phase $\theta = \omega t$ at a distance R. The observer is to the right of this system in the $\hat{x}$-direction. $\hat{o}$ is the direction from the system to the location of the observer and in this system equal to $\hat{x}$. The observer's view is edge-on. The figure is not to scale.*

In this system, the planet travels in orbit around the star. At time t, the angle with orbital angular frequency ω between the position of the planet and the x-axis is $\theta = \omega t$. As the orbit is circular, the position vector of the planet is

$$\vec{R}(t) = R \begin{pmatrix} \cos(\omega t) \\ \sin(\omega t) \\ 0 \end{pmatrix} \tag{2.1}$$

Initially at $t = 0$, $\vec{R} = R\hat{x}$. We assume the system is observed from far away by an observer in the $\hat{x}$-direction. The normalized vector $\hat{o}$ indicates the direction from the system towards the observer. We will take $\hat{o} = \left(1, 0, 0\right)^T$ or $\hat{o} = \hat{x}$, unless stated otherwise (see figure 2.1).
We assume that the planet is a sphere with a homogeneous surface. This means that the planet looks the same from all viewing directions, so that rotation does not play a roll anymore. Furthermore, we assume Lambertian reflection. Lambertian reflection is a property of a surface that scatters the light from any incident direction into all viewing directions equally [14]. This means the brightness of the surface is the same from all viewing directions. We also assume that $S + s \ll R$ and thus that

$$S \ll R \tag{2.2}$$

and

$$s \ll R \tag{2.3}$$

2.2 Phases

Exoplanets are too far from Earth to be observed directly. Astronomers can only observe a total light signal, which consists of the light from the star in the direction of the observer plus the light reflected by the planet towards the observer. The light signal by the star we take a constant. The light signal reflected by the planet varies due to phases. For example, the sun always illuminates half of the moon's surface, so from the Sun's point of view you would always see a full moon. On Earth we don't always see a full moon in the sky due to phases. Sometimes we see a crescent or a new moon, as in figure 2.2.

Figure 2.2: *A figure of the crescent moon, a phase of the moon.*

Exoplanets can be studied by analyzing the reflected light signal and thus analyzing the phases. In order to calculate the reflected light signal at a time t in the system discussed in section 2.1, we need to know what part of light that falls on the surface is reflected to the observer. For this, we introduce the vectors $\hat{s}(\mu,\nu)$ and $\hat{R}(t)$. $\hat{s}(\mu,\nu)$ is the normalized vector of $\vec{s}(\mu,\nu)$, the vector from the center of the planet to a point on the surface of the planet:

$$\vec{s}(\mu,\nu) = s\begin{pmatrix}\cos(\mu)\sin(\nu)\\ \sin(\mu)\sin(\nu)\\ \cos(\nu)\end{pmatrix} = s\hat{s} \tag{2.4}$$

There μ is the azimuthal angle and ν is the polar angle of the spherical coordinates. So $0 \leq \mu < 2\pi$ and $0 \leq \nu \leq \pi$. $\hat{R}(t)$ is the normalized vector from the origin of the star to the planet, so the normalized vector of $\vec{R}(t)$.

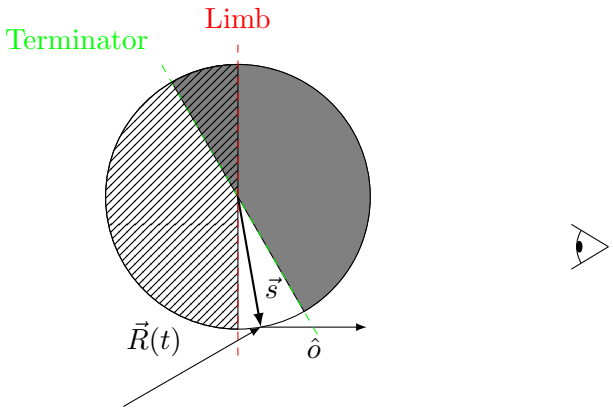

Figure 2.3: *An enlargement of the planet from figure 2.1. $\vec{R}(t)$ is the vector from the center of the star to a point on the surface, $\vec{s}$ the vector from the center of the planet that points to the surface of the planet and $\hat{o}$ is the unit-vector towards the observer. The illuminated part of the planet is the white area, the dark part is the gray area. The invisible part of the planet by the observer is indicated with stripes. The terminator is the border between the illuminated and the dark part of the planet and the limb the border between the visible and invisible part of the planet. In this figure, the observer will observe a crescent shown in figure 2.2.*

In figure 2.3 we see an enlargement of the planet in figure 2.1. We see how the planet is divided in different parts. We have a distinction between the illuminated part and the dark part where no light reaches the surface of the planet. There is also a distinction between the part visible and invisible to the observer.
The white area is the illuminated part of the planet. For a point $\vec{s}(\mu,\nu)$ to lie in this part, the angle between $\vec{R}(t)$ and $\vec{s}(\mu,\nu)$ must be larger than 90°. This is the part of the surface where $\vec{R}(t)\cdot\vec{s}(\mu,\nu) \leq 0$. The grey area is the dark part. For a point $\vec{s}(\mu,\nu)$ to lie in this part, the angle between $\vec{R}(t)$ and $\vec{s}(\mu,\nu)$ should be smaller than 90°. This is the part where $\vec{R}(t)\cdot\vec{s}(\mu,\nu) \geq 0$. The border between these parts is called the terminator. On this curve, $\vec{R}(t)\cdot\vec{s}(\mu,\nu) = 0$.
The planet is also divided parts that are visible and invisible to the observer. The visible part in figure 2.3 is not striped. A point $\vec{s}(\mu,\nu)$ on the surface of the planet lies in the visible part if the angle between the vectors $\vec{s}(\mu,\nu)$ and $\hat{o}$ is smaller than 90°. This is given as $\vec{s}(\mu,\nu)\cdot\hat{o} \geq 0$. The invisible part is depicted in figure 2.3 as striped. A point $\vec{s}(\mu,\nu)$ on the surface of the planet lies in the invisible part if the angle between the vectors $\vec{s}(\mu,\nu)$ and $\hat{o}$ is larger than 90°. This is given as $\vec{s}(\mu,\nu)\cdot\hat{o} \leq 0$. The border between the visible and invisible part of the planet is called the Limb, this is where $\vec{s}(\mu,\nu)\cdot\hat{o} = 0$.
With these findings, we come to the conclusion that the observer sees light on the following region of the planet surface:

$$\mathfrak{D} = \{\vec{s}(\mu,\nu)\cdot\hat{o} \geq 0 \wedge \vec{s}(\mu,\nu)\cdot\vec{R}(t) \leq 0\} \tag{2.5}$$

These conditions change over time and lead to the phases of the planet in figure 2.4. When the planet is fully lit observed (left in figure 2.4), then $\mathfrak{D}$ is a hemisphere.

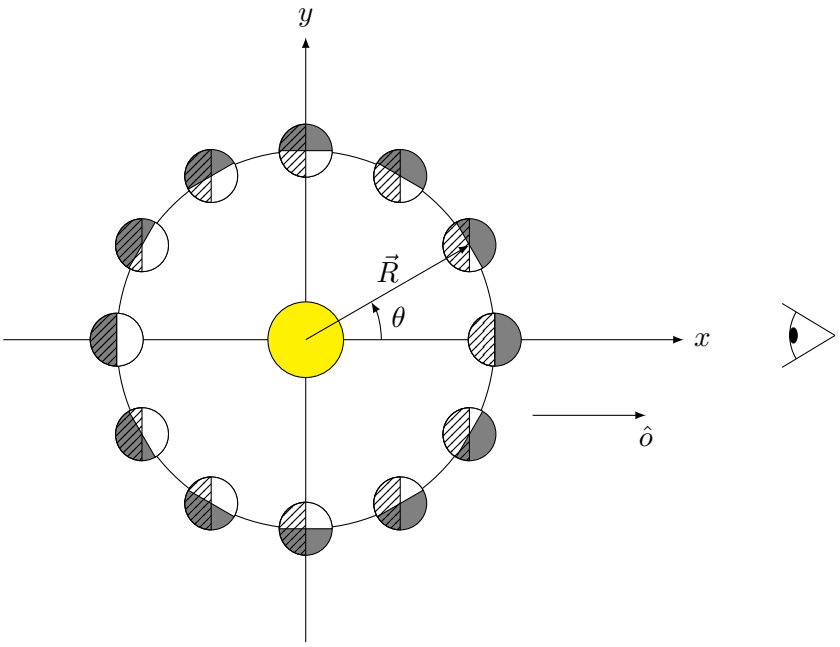

Figure 2.4: *Some possible phases of a planet. The phases of the planet depend directly on the phase angle θ. The planets positioned at $R\hat{x}$, $R\hat{y}$, $-R\hat{x}$ and $-R\hat{y}$ are in phases called 'new moon', 'first quarter', 'full moon' and 'last quarter' respectively. The star is located in the origin. The observer is in the $\hat{x}$-direction. The observer's view is edge-on. The figure is depicted face-on (top view), and is not to scale.*

2.3 Reflected light signal

In this thesis we want to calculate the reflected light signal from the planet to the observer. The reflected light signal we will call $f(t)$ and is given as:

$$f(t) = \frac{s^2}{\pi R^2} \iint_{\mathbb{D}} (-\hat{R}(t) \cdot \hat{s}(\mu, \nu))(\hat{s}(\mu, \nu) \cdot \hat{o}) \sin(\nu) d\mu d\nu \tag{2.6}$$

We now will derive expression in 2.6.
Imagine the star in the system has total power output P_0, see figure 2.5.

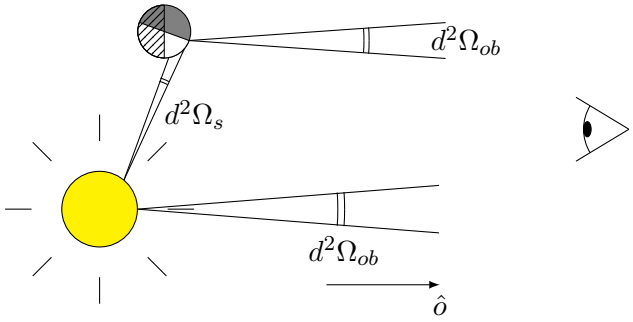

Figure 2.5: *The system of figure 2.1. $d^2\Omega_{ob}$ is the solid angle of a point on the surface of the star or planet in the direction of the observer. $d^2\Omega_s$ is the solid angle of a point on the surface of the star towards the planet. The eye indicates the observers point of view. It is not a problem that the eye is apparently larger than the star.*

Consider the direct light from the star. The by the observer received total power P_{ob} is a fraction of the total emitted power P_0. We only take in consideration the fraction emitted in the direction of the observer, so in the direction of the solid angle $d^2\Omega_{ob}$. In spherical coordinates, the solid angle is equal to $d^2\Omega_{ob} = \sin(\theta) d\theta d\phi$. The received power P_{ob} becomes:

$$P_{ob} = P_0 \frac{d^2\Omega_{ob}}{\int d^2\Omega_{ob}} = P_0 \frac{d^2\Omega_{ob}}{4\pi} \tag{2.7}$$

Next we calculate the light reflected by the planet towards the observer. We consider a small surface element on the planet $d\vec{S}$. This vector is oriented outwards. We use the notation for a solid angle on the planet as seen from the center of the planet

$$d^2\Omega_s = \sin(\nu) d\mu d\nu \tag{2.8}$$

in the spherical coordinates of the planet surface. Hence, $d\vec{S}$ (see figure 2.6) will be equal to

$$d\vec{S} = s^2 \hat{s} (d^2\Omega_s) = s^2 \hat{s} \sin(\nu) d\mu d\nu \tag{2.9}$$

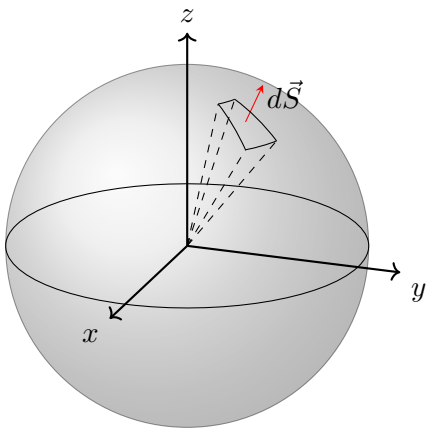

Figure 2.6: *The planet surface. $d\vec{S}$ is a small surface area of the planet.*

This surface element receives power

$$P_s = P_0 \frac{(-\hat{R}(t) \cdot d\vec{S})}{4\pi R^2} \tag{2.10}$$

using the inverse-square law. An observer will only intercept a fraction $d^2\zeta$ of P_s, namely the fraction in the direction of the observer

$$d^2\zeta = \frac{(\hat{o} \cdot \hat{s})}{\pi} d^2\Omega_{ob} \tag{2.11}$$

Then the total observed power at the reflected surface element $d\vec{S}$ on the planet equals the product of equation 2.10 with equation 2.11:

$$P_s d^2\zeta = \frac{P_0 s^2}{4\pi^2 R^2} (-\hat{R}(t) \cdot \hat{s})(\hat{o} \cdot \hat{s}) d^2\Omega_s d^2\Omega_{ob} \tag{2.12}$$

We compare this result with the power from the star (equation 2.7). Hence, relative to the star the intensity from $d\vec{S}$ is

$$\frac{P_s d^2\zeta}{P_{ob}} = \frac{s^2}{\pi R^2} (-\hat{R}(t) \cdot \hat{s})(\hat{o} \cdot \hat{s}) d^2\Omega_s \tag{2.13}$$

If we integrate equation 2.13 over the full planet surface, we obtain equation 2.6, the equation for the reflected light signal. The same result is found in [11] as equation 6. The only difference is the assumption that the planet is not homogeneous in [11]. Equation 6 gets an extra mapping term $M(\hat{s}, t)$ in [11]. In equation 2.6 this factor is 1 (homogeneous planet). There is also a small difference in normalization. It remains to be shown that 2.11 is true. This we show by integrating over all reflected directions in space

$$\iint \frac{\hat{o} \cdot \hat{s}}{\pi} d^2\Omega_{ob} = \frac{1}{\pi} \int_0^{2\pi} \int_0^{\frac{\pi}{2}} \cos(\phi) 1^2 \sin(\phi) d\phi d\theta = \frac{1}{\pi} \cdot 2\pi \cdot \frac{1}{2} = 1 \tag{2.14}$$

where ϕ is the polar angle, θ the azimuthal angle, $1^2 \sin(\phi)$ is the Jacobian of the integral.

2.4 Results

Equation 2.6 for the reflected light signal is programmed in MATLAB, see Appendix A. The integral is calculated with the following Riemann sum

$$f(t) \approx \frac{s^2}{\pi R^2} \frac{2\pi}{N_\mu} \frac{\pi}{N_\nu} \sum_{\mathcal{D}} \big(- \hat{R}(t) \cdot \hat{s}(\mu_k, \nu_l) \big) \big(\hat{s}(\mu_k, \nu_l) \cdot \hat{o} \big) \sin(\nu_l) \tag{2.15}$$

where N_μ the number of points in μ, N_ν the number of points in ν, μ_k the k^{th} value in μ and ν_l the l^{th} value in ν. The summation for k is from 0 to $N_\mu - 1$ and for l from 0 to $N_\nu - 1$, constraint to the lune $\mathcal{D}$. Hereby we have a Riemann sum for the surface integral.
We calculate the integral (2.15) for one planet. The result is the graph in figure 2.7.

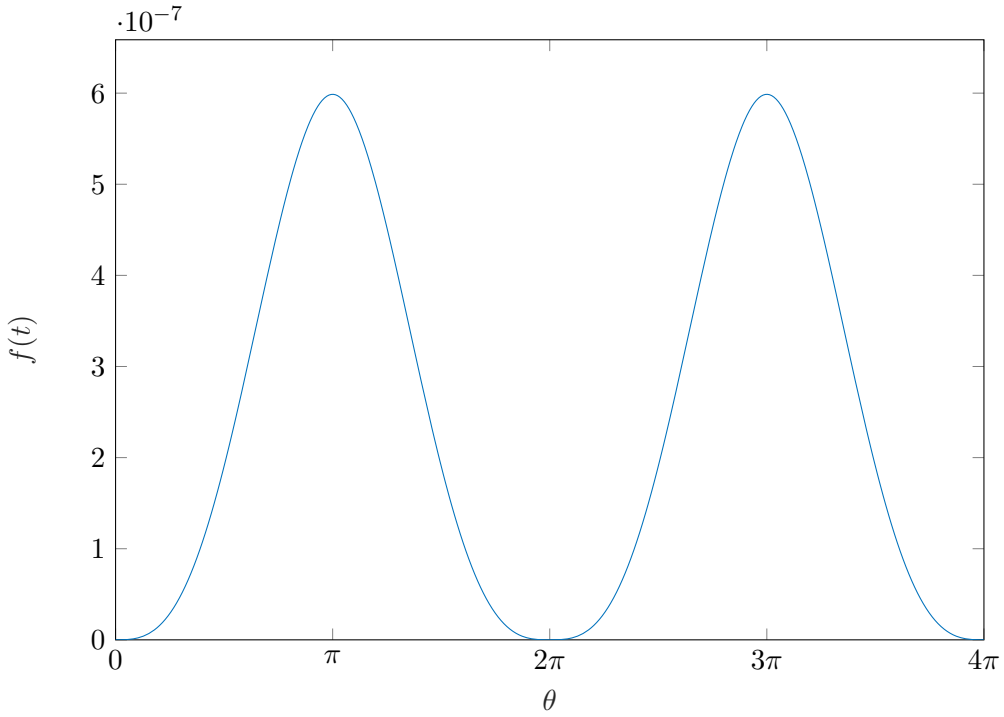

Figure 2.7: *The reflected light signal for one planet using equation 2.15. Here we see the reflected light for two full orbits or from $\omega t = 0$ until $\omega t = 4\pi$. At $\omega t = \pi$, there is a maximum. This occurs because the planet is observed fully illuminated.*

This is a smooth and periodic curve in the orbital phase $\theta = \omega t$. We clearly see the differences in the phases of the exoplanet in the reflected light signal. When $\theta = \pi + 2\pi k$ for $k \in \mathbb{Z}$, the phase of the planet is 'full moon' and a maximum should occur. The opposite phase is $\theta = 2\pi k$ for $k \in \mathbb{Z}$. At these values of θ, the phase is 'new moon', so here we expect a minimum. In between we expect a continuous process of the reflected light signal by the phases of the planet. We see that the light signal is an even function around 0.

3 Planet-Binary system

In the previous chapter we have described the reflected light signal for a system with one planet. In this chapter an extra body is added to the system, so that we have a system with a planet with companion. We will examine the effect on the reflected light signal by examining eclipses on both bodies. The occurrence and the duration of an eclipse is examined. Furthermore, the radii of the bodies is varied to examine the effect on the reflected light signal.

3.1 Theory

We will look at a system of a star and two bodies orbiting around the star. The center of mass of the two orbiting bodies lies at a certain distance R from the star, see figure 3.1.

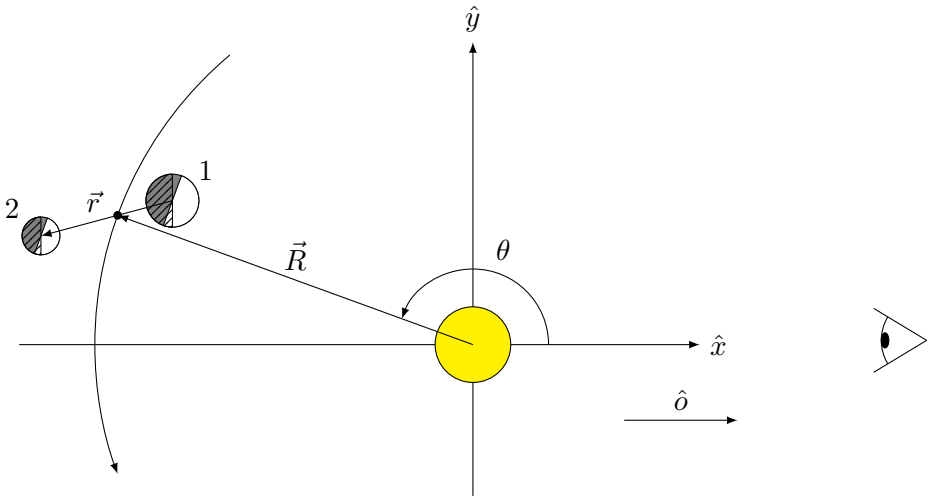

Figure 3.1: *A figure of the binary planet system. The figure is depicted face-on (top view). The star is located in the origin. The barycenter of the two bodies orbits around the star in a circular orbit in the xy-plane with phase $\theta = \omega t$ at a distance R from the star. $\vec{r}$ is the relative vector between the planet and the moon, which orbits with phase $\phi = \Omega t$. The observer $\hat{o}$, is in the $\hat{x}$-direction. The observer's view is edge-on. The figure is not to scale.*

We have the two bodies, which we will call planet 1 and planet 2. These have respective positions $\vec{R}_1$ and $\vec{R}_2$, masses m_1 respectively m_2 and radii s_1 respectively s_2. We will assume that $s_1 \geq s_2$, so we will call planet 1 'the planet' and planet 2, 'the moon'. The position of the barycenter $\vec{R}$ is given by [13]

$$\vec{R} = \frac{m_1\vec{R}_1 + m_2\vec{R}_2}{m_1 + m_2} \tag{3.1}$$

The vector from the planet to the moon which describes the relative motion is called the relative vector:

$$\vec{r} = \vec{R}_2 - \vec{R}_1 \tag{3.2}$$

Equation 3.1 and 3.2 combined will give an expression for $\vec{R}_1$ and $\vec{R}_2$:

$$\vec{R}_1 = \vec{R} - \frac{m_2\vec{r}}{m_1 + m_2} \tag{3.3}$$

$$\vec{R}_2 = \vec{R} + \frac{m_1\vec{r}}{m_1 + m_2} \tag{3.4}$$

The motion of a planet around a star lies in a plane [13]. We choose $\vec{R}$ such that the barycenter orbits the star at a certain distance R in a circular plane. Then

$$\vec{R} = R \begin{pmatrix} \cos(\omega t) \\ \sin(\omega t) \\ 0 \end{pmatrix} \tag{3.5}$$

We assume that $\vec{r}$ is a rotating vector, describing a circular motion around the barycenter

$$\vec{r} = r \begin{pmatrix} \cos(\Omega t) \\ \sin(\Omega t) \\ 0 \end{pmatrix} \tag{3.6}$$

Here $|\vec{r}| = r$ is the distance between the planet and the moon and where Ω is the rotational frequency. No inclination between the planets is assumed. Hence the two planets move according to

$$\vec{R}_1(t) = R \begin{pmatrix} \cos(\omega t) \\ \sin(\omega t) \\ 0 \end{pmatrix} - \frac{m_2 r}{m_1 + m_2} \begin{pmatrix} \cos(\Omega t) \\ \sin(\Omega t) \\ 0 \end{pmatrix} \tag{3.7}$$

$$\vec{R}_2(t) = R \begin{pmatrix} \cos(\omega t) \\ \sin(\omega t) \\ 0 \end{pmatrix} + \frac{m_1 r}{m_1 + m_2} \begin{pmatrix} \cos(\Omega t) \\ \sin(\Omega t) \\ 0 \end{pmatrix} \tag{3.8}$$

The initial situation (at $t = 0$) will be aligned with the star in the $\hat{x}$-direction.

$$\vec{R}_1(0) = \begin{pmatrix} R - \frac{m_2 r}{m_1 + m_2} \\ 0 \\ 0 \end{pmatrix} \tag{3.9}$$

$$\vec{R}_2(0) = \begin{pmatrix} R + \frac{m_1 r}{m_1 + m_2} \\ 0 \\ 0 \end{pmatrix} \tag{3.10}$$

At that moment, the star, the planet and the moon are aligned and the planet is in between the star and the moon. At $t = 0$, there is an eclipse, which will be explained in section 3.2.

3.2 Eclipses and occultations

In the system described in paragraph 3.1 eclipses and occultations can occur. An eclipse is an occurrence where one body blocks the light falling on a second body. An occultation is an occurrence where a body blocks the reflected light from a second body to an observer. Searching for eclipses can be a method for discovering exomoons, because eclipses do not occur in a system with only one planet.
An eclipse can occur in the system described in paragraph 3.1, when the moon (the planet) is in between the planet (the moon) and the star and all are aligned. In figure 3.2, we see a representation of an eclipse on the Earth. A cone named the umbra is the area of total eclipse, the penumbra is the area of partial eclipse. For a total eclipse to happen like in figure 3.3, the planet has to be positioned exactly in the cone. The height h of the cone is described by equation (A4) in [4].

$$h = S\left(\frac{R_2}{S - s_2} - \frac{S - s_2}{R_2}\right) \tag{3.11}$$

At the moment of an eclipse, we can assume that $\vec{R}_2 \approx \vec{R}$. We assumed in paragraph 2.1 that $S \ll R$ (2.2) and $s \ll R$ (2.3) so $s_2 \ll R$, in this case $h \to \infty$. In this case the cone becomes a cylinder. The rays travel parallel to the planet.
We will explain the situation when the moon is in between the star and the planet, see figure 3.3. The vector that points from the star to the moon is $\vec{R}_2$. Behind the moon, there exists an infinite cylinder

where all the light is blocked. In this cylinder, $\vec{R}_2$ is the symmetry axis through the flat bottom and backs of the cylinder. We assumed $\vec{R}_2 \approx \vec{R}$, so $\vec{R}$ is approximately the symmetry axis of the shadow cylinder.

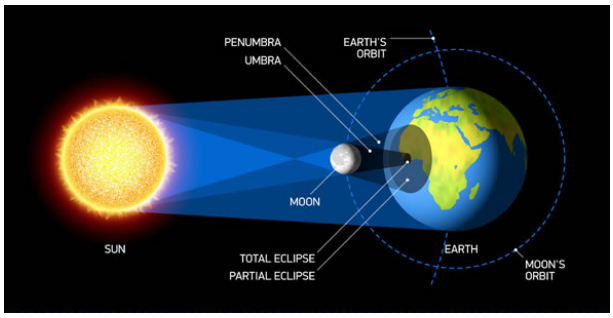

Figure 3.2: *A figure of an eclipse on the Earth caused by the Moon passing between the Sun and the Earth [15]. The Sun shines light towards the Earth. The light is blocked by the Moon. The penumbra is the area where the light is totally blocked, so a total eclipse occurs. The umbra is the area where the sun is partially blocked by the Moon, so a partial eclipse occurs. In this figure, clearly the conditions 2.2 and 2.3 do not hold.*

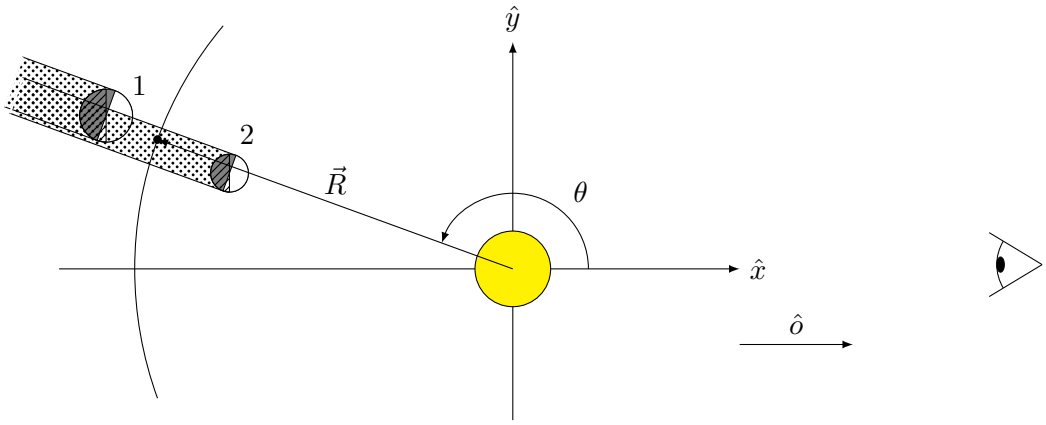

Figure 3.3: *A representation of an eclipse on the planet by the moon. The star is in the origin. The barycenter is placed at phase $\theta = \omega t$ at a distance R. The dotted area is the shadow cylinder behind the moon and behind the planet with symmetry axis $\vec{R}$. The planet lies partly in the shadow cylinder behind the moon, thus the area on the surface of the planet in the cylinder is where the eclipse occurs. The observer is placed in the positive $\hat{x}$-direction. The figure is depicted face-on (top-view).*

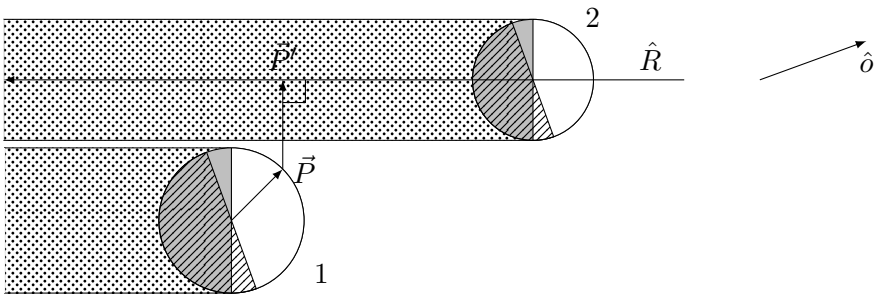

Figure 3.4: *An enlargement of the planet and the moon in figure 3.3. A point $\vec{P}$ on the surface of the planet is specified. $\vec{P}'$ is the orthogonal projection of $\vec{P}$ on $\hat{R}$. The dotted area is the shadow cylinder of the moon or the planet. The symmetry axis $\hat{R}$ of the cylinder is displayed.*

How do we know if the planet is located in the shadow cylinder of the moon? There are two conditions. First, the planet has to be further away from the star than the moon. This happens when

$$|\vec{R}_1| \geq |\vec{R}_2| \tag{3.12}$$

Second, we have to look at $d(\vec{P}, \vec{P}')$, the distance from $\vec{P}$ to $\vec{P}'$, in figure 3.4. $\vec{P}$ is a point on the surface of the planet

$$\vec{P} = \vec{R}_1 + \vec{s}_1 = \vec{R}_1 + s_1\hat{s}(\mu, \nu) \tag{3.13}$$

where $\vec{s}_1$ is the vector from the center of the planet to $\vec{P}$. $\vec{P}'$ is the orthogonal projection of $\vec{P}$ on $\vec{R}$. The point $\vec{P}$ on the surface of the planet touches the cylinder if $d(\vec{P}, \vec{P}') = s_2$. So if $d(\vec{P}, \vec{P}') \leq s_2$, the point on the surface lies within the cylinder. $\vec{P}'$ is equal to

$$\vec{P}' = \frac{\vec{P} \cdot \vec{R}_2}{\vec{R}_2 \cdot \vec{R}_2}\vec{R}_2 = \frac{\vec{P} \cdot \vec{R}_2}{|\vec{R}_2|^2}\vec{R}_2 = (\vec{P} \cdot \hat{R}_2)\hat{R}_2 \tag{3.14}$$

$\hat{R}_2$ is the normalized vector of $\vec{R}_2$. Then the distance $d(\vec{P}, \vec{P}')$ is

$$d(\vec{P}, \vec{P}') = |\vec{P} - (\vec{P} \cdot \hat{R}_2)\hat{R}_2| = \sqrt{|\vec{P}|^2 - |\vec{P} \cdot \hat{R}_2|^2} = \sqrt{|\vec{P}|^2|\hat{R}_2|^2 - |\vec{P} \cdot \hat{R}_2|^2} = |\vec{P} \times \hat{R}_2| \tag{3.15}$$

where the Lagrange's identity is used in the last step (because $|\hat{R}_2| = 1$). Equation 3.15 we can write as

$$|\vec{P} \times \hat{R}_2| = |(\vec{R}_2 - \vec{r} + \vec{s}_1) \times \hat{R}_2| = |\vec{R}_2 \times \hat{R}_2 + (-\vec{r} + \vec{s}_1) \times \hat{R}_2| = |(-\vec{r} + \vec{s}_1) \times \hat{R}_2| \tag{3.16}$$

In the assumption that $\vec{R}_2 \approx \vec{R}$, we conclude

$$d(P, P') = |(-\vec{r} + \vec{s}_1) \times \hat{R}_2| \approx |(-\vec{r} + \vec{s}_1) \times \hat{R}| \leq s_2 \tag{3.17}$$

The condition for an eclipse will now be given by combining the two conditions 3.12 and 3.17:

$$\big(d(\vec{P}, \vec{P}') = |\vec{P} \times \hat{R}_2| \approx |(-\vec{r} + \vec{s}_1) \times \hat{R}| \leq s_2\big) \wedge \big(|\vec{R}_1| \geq |\vec{R}_2|\big) \tag{3.18}$$

The same derivation holds for an eclipse on the moon by the planet and will give as result:

$$\big(d(\vec{P}, \vec{P}') = |\vec{P} \times \hat{R}_1| \approx |(\vec{r} + \vec{s}_2) \times \hat{R}| \leq s_1\big) \wedge \big(|\vec{R}_1| \leq |\vec{R}_2|\big) \tag{3.19}$$

3.3 Occurrence of an eclipse

A total eclipse on the moon occurs when the axes $\hat{R}$ and $\hat{r}$ are aligned. If the planet is in between the star and the moon, we get

$$\begin{aligned} \hat{r} &= \hat{R} && \Leftrightarrow \\ \begin{pmatrix} \cos(\Omega t) \\ \sin(\Omega t) \\ 0 \end{pmatrix} &= \begin{pmatrix} \cos(\omega t) \\ \sin(\omega t) \\ 0 \end{pmatrix} && \Leftrightarrow \\ \Omega t &= \omega t + 2\pi n && \Leftrightarrow \\ \hat{t}_n &= \frac{2\pi n}{\Omega - \omega} \end{aligned}$$

for any $n \in \mathbb{Z}$. The time $\hat{t}_n$ is the time of total eclipse. Total eclipses also occur when the moon is in between the planet and the star, see figure 3.3. In that case, $\hat{r} = -\hat{R}$. This gives a phase shift so $\tilde{t}_n = \frac{\pi + 2\pi n}{\Omega - \omega}$. We conclude that any total eclipse happens when

$$t_n = \frac{\pi n}{\Omega - \omega} \tag{3.20}$$

3.4 Duration of an eclipse

We now derive the condition for the duration of an eclipse. Because of assumption 2.3, we can take $\vec{R}_1 \approx \vec{R}_2 \approx \vec{R}$, so $\hat{R}_1 \approx \hat{R}_2 \approx \hat{R}$. That's why figure 3.4 can also be pictured as

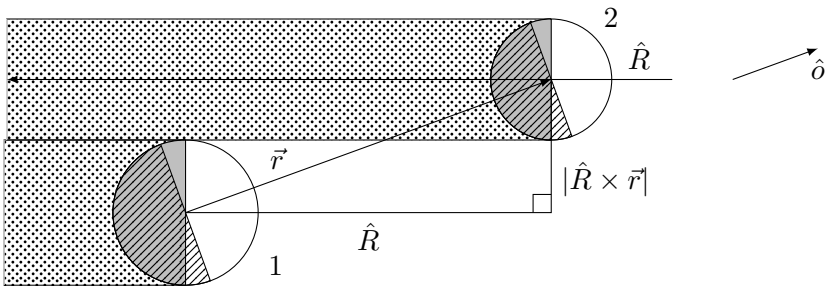

Figure 3.5: *An image of an ending eclipse. The moon moves from in between the planet and the star away from there. The dotted area is the shadow cylinder of the moon or the planet, where $\hat{R}$ is the symmetry axis. The distance between the symmetry axes of the planet and the moon is $|\hat{R} \times \vec{r}|$ or $s_1 + s_2$. The same derivation can be done for a starting eclipse.*

Here we see that at the start and the end of an eclipse, $\left|\vec{r} - \big(\vec{r} \cdot \hat{R}\big)\hat{R}\right| = s_1 + s_2$.

$$\begin{aligned} \left|\vec{r} - \big(\vec{r} \cdot \hat{R}\big)\hat{R}\right| = \left|\big(1 - \hat{R}\hat{R}\big) \cdot \vec{r}\right| &= s_1 + s_2 && \Leftrightarrow \\ \left|\big(R - \vec{R}\hat{R}\big) \cdot \vec{r}\right| = \sqrt{R^2 r^2 - (\vec{r} \cdot \vec{R})^2} &= R\big(s_1 + s_2\big) && \Leftrightarrow \\ \left|\vec{R} \times \vec{r}\right| &= R\big(s_1 + s_2\big) && \Leftrightarrow \\ \left| \begin{pmatrix} \cos(\omega t) \\ \sin(\omega t) \\ 0 \end{pmatrix} \times r \begin{pmatrix} \cos(\Omega t) \\ \sin(\Omega t) \\ 0 \end{pmatrix} \right| &= s_1 + s_2 && \Leftrightarrow \\ \sqrt{\big(\cos(\omega t)\sin(\Omega t) - \cos(\Omega t)\sin(\omega t)\big)^2} &= \frac{s_1 + s_2}{r} && \Leftrightarrow \\ \sqrt{\sin^2((\Omega - \omega)t)} = \big|\sin((\Omega - \omega)t)\big| &= \frac{s_1 + s_2}{r} \end{aligned}$$

We linearize this expression around the time of total eclipses t_n (3.20), so $t_n = \frac{\pi n}{\Omega-\omega} + dt$, this gives for small dt

$$\begin{aligned} \big|\sin\big((\Omega-\omega)t_n\big)\big| = \big|\sin\big((\Omega-\omega)dt\big)\big| = (\Omega-\omega)dt \quad &\Leftrightarrow \\ \big|\sin((\Omega-\omega)t)\big| = (\Omega-\omega)|dt| = \frac{s_1+s_2}{r} \quad &\Leftrightarrow \\ dt = \pm\frac{s_1+s_2}{(\Omega-\omega)r} \end{aligned}$$

Hence, the nth eclipse lies in the interval:

$$\frac{\pi n}{\Omega-\omega} - \frac{s_1+s_2}{(\Omega-\omega)r} < t_n < \frac{\pi n}{\Omega-\omega} + \frac{s_1+s_2}{(\Omega-\omega)r} \tag{3.21}$$

The total duration of one eclipse is equal to

$$2|dt| = \frac{2(s_1+s_2)}{(\Omega-\omega)r} \tag{3.22}$$

3.5 Occultations

In paragraph 3.2 we mentioned occultations. An occultation is an occurrence where a body blocks the reflected light from a second body to an observer. We will evaluate the event where the moon is in between the planet and the observer, see figure 3.6.

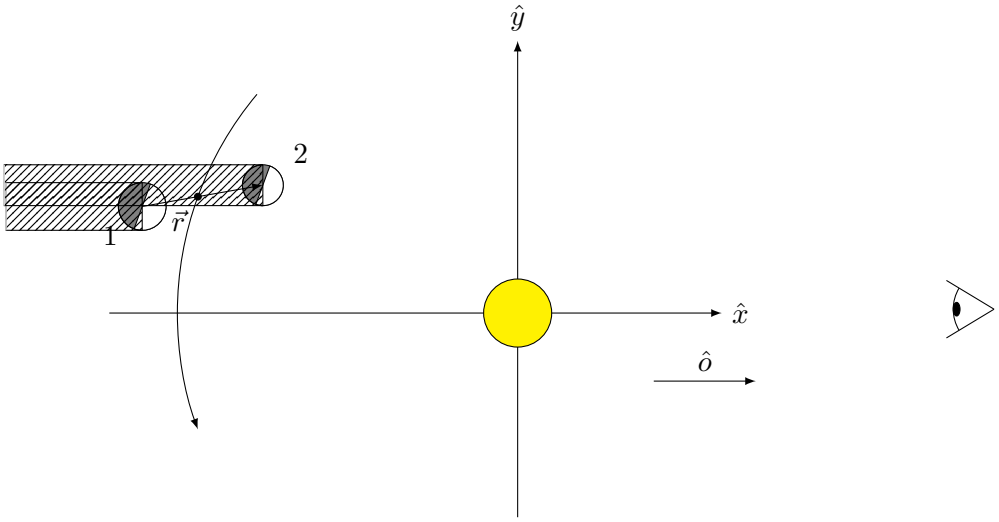

Figure 3.6: *An image of an occultation. The moon is in between the planet and the observer. The striped areas are the cylinders behind the planet and the moon, where the observer cannot see. The observer is in the $\hat{x}$-direction.*

In figure 3.6, the observer cannot see behind the moon. We approximate the space behind the moon with a cylinder with symmetry axis $\hat{o}$. At the time of an occultation, the surface area of the planet located in the cylinder is not contributing to the light signal. The condition for the surface area to be in the cylinder, can be derived the same way as for an eclipse in paragraph 3.2. Take a point $\vec{P}$ on the surface of the planet, project the point on $\hat{o}$, and check if $d(\vec{P},\vec{P}') \leq s_2$. If the derivation in paragraph 3.2 is followed for this case, we get $d(\vec{P},\vec{P}') = |\vec{P}\times\hat{o}|$.
It also has to be checked that the moon is closer to the observer than the planet. This we will do by evaluating $(\vec{R}_2 - \vec{R}_1)\cdot\hat{o}$ or $\vec{r}\cdot\hat{o}$. If this value is larger than zero, the moon is closer to the observer

than the planet.
The conditions for an occultation (the moon is in between the observer and the planet) are

$$\left(|\vec{P} \times \hat{o}| \leq s_2\right) \wedge \left((\vec{R}_2 - \vec{R}_1) \cdot \hat{o} > 0\right) \tag{3.23}$$

The condition for when the planet is in between the observer and the moon is derived in the same way and that gives:

$$\left(|\vec{P} \times \hat{o}| \leq s_1\right) \wedge \left((\vec{R}_1 - \vec{R}_2) \cdot \hat{o} > 0\right) \tag{3.24}$$

This condition is not being implemented in the MATLAB code, because we assume there is a slight observer inclination (see section 5) ensuring that occultations never happen.

3.6 Reflected light signal for the planet-binary system

In paragraph 2.1 we saw that the reflected light signal from one planet could be evaluated by calculating the integral in equation 2.6. An astronomer cannot separate the two bodies in the planet-binary system with his telescope. He can only observe the total reflected light signal $f_B(t)$. Therefore we calculate the total light signal of the system. To do this for the binary system, we can modify equation 2.6.
For the system with two bodies, we express the total reflected light signal as a sum of contributions from the two individual bodies. We use the integral in equation 2.6 separately on both bodies and add the result:

$$f_B(t) = f_1(t) + f_2(t) \tag{3.25}$$

where $f_1(t)$ is the contribution from the planet and $f_2(t)$ is the contribution from the moon.

3.7 Results for eclipses in time domain

In this section we calculate the total reflected light signal f_B (3.25) of the planet-binary system described in paragraph 3.1 with the MATLAB code in Appendix B. We take in consideration condition 2.5 for the phases of the bodies and conditions 3.18 and 3.19 for eclipses on the bodies.
First we will study the contributions of the separate bodies, the reflected light signals f_1 and f_2, with $s_1 = s_2 = R_{Jup}$. The result is depicted in figure 3.7.

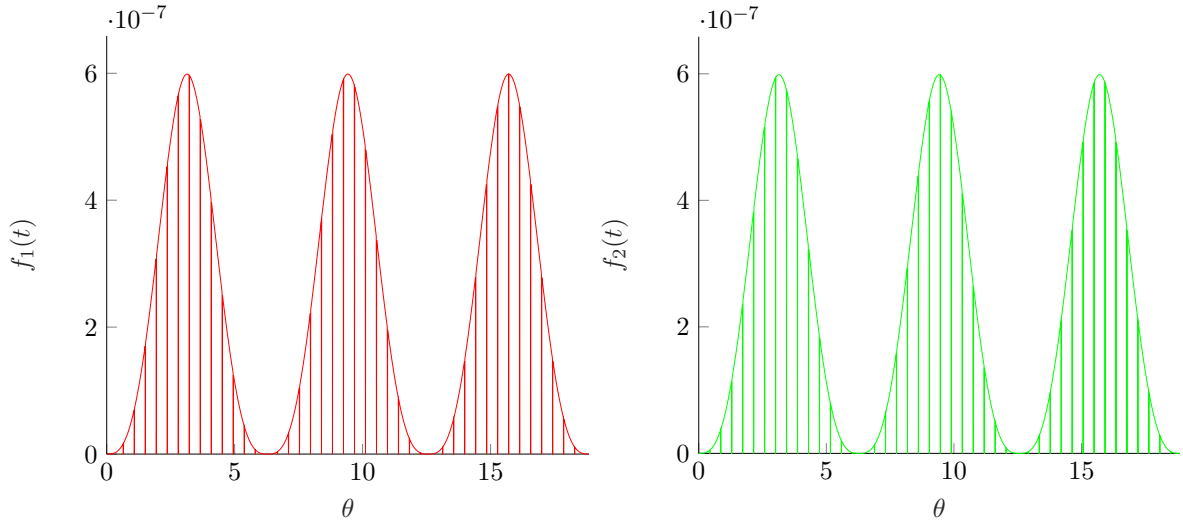

(a) *Reflected light signal* f_1 **(b)** *Reflected light signal* f_2

Figure 3.7: *The reflected light signals* f_1 *(3.7a) and* f_2 *(3.7b) plotted against* θ *for* $s_1 = s_2 = R_{Jup}$ *in red and green respectively. The figures have the same shape as the reflected light signal of a system with one planet, but with additional jumps to zero. These jumps to zero illustrate total eclipses on the surface of that body. We see that figure 3.7a and figure 3.7b are almost the same (because the planet and moon have the same radius) except for a phase change in the delta peaks. Three orbits of the barycenter around his host star are plotted in this figure.*

The shape of the reflected light signals f_1 and f_2 look the same as the reflected light signal of a system with one planet (2.7), but in f_1 and f_2 are jumps to zero. Every time a jump occurs, a total eclipse occurs on that planet. A phase shift exists between the peaks of the reflected light signals f_1 and f_2. This effect can be explained by the fact that if a total eclipse occurs on the planet, there cannot occur an eclipse on the moon by condition 3.18. The other body must be fully illuminated by the star.
If the two signals in figure 3.7 are added, the total reflected light signal is obtained, see figure 3.8. The total reflected light signal $f_B(t)$ also has the shape of the reflected light signal of one planet, but is twice as high as one planet for two equal-size bodies. This agrees with equation 3.25. Jumps also occur here, but these go to half the current value of the signal. Always one of the bodies must be illuminated by the sun, so a signal is always obtained, which corresponds to this offset. Note how the offset is exactly the signal of one body. Also note that the signal is almost periodic. The shape remains the same, but the jumps (eclipses) are not on the same places in each orbit. So the signal is quasi-periodic.

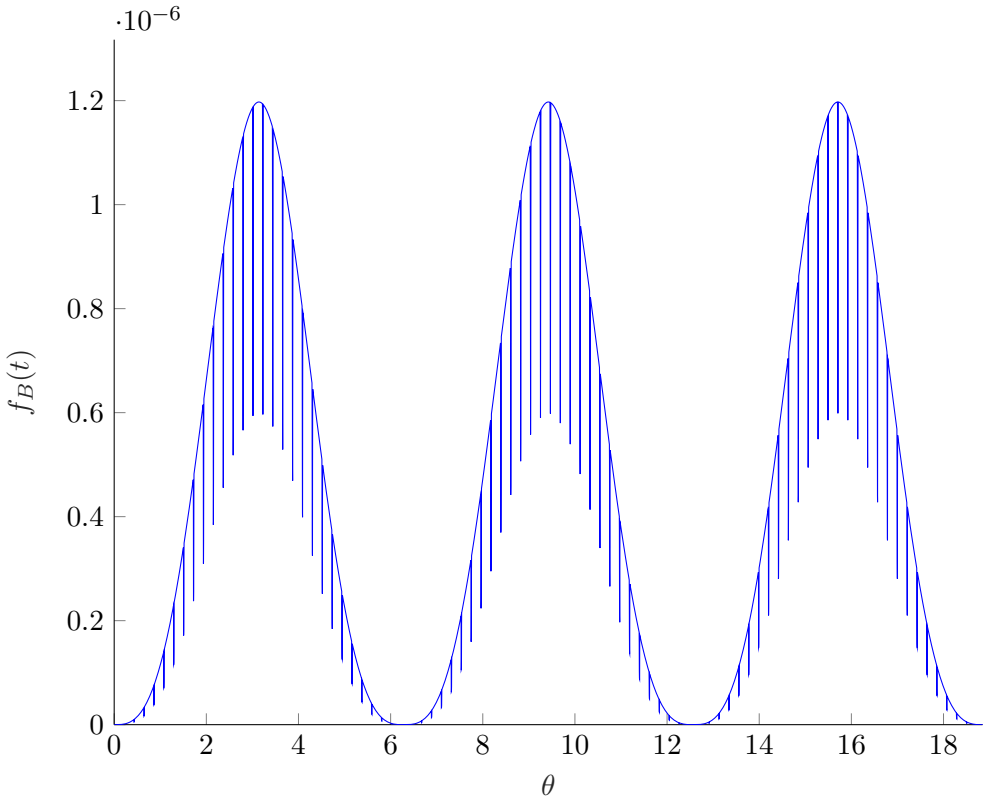

Figure 3.8: *The total reflected light signal f_B plotted against θ for a system with two bodies with $s_1 = s_2 = R_{Jup}$. Three orbits of the barycenter around the star are plotted in this figure. Every time an eclipse occurs, a sharp dip in the reflected light signal is seen.*

An astronomer will only observe the signal in figure 3.8, because the astronomer cannot separate the different signals. If we zoom in on one of the jumps of the signal around $\theta = \frac{1}{2}\pi$, on one around $\theta = \pi$ and on one around $\theta = \frac{3}{2}\pi$ in figure 3.8, we will see the signals in figure 3.9.

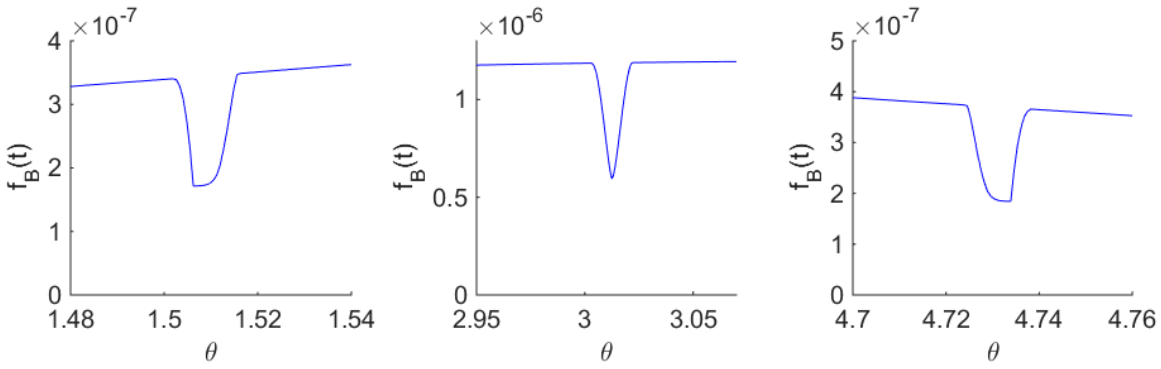

(a) *An eclipse around* $\theta = \frac{1}{2}\pi$. **(b)** *An eclipse around* $\theta = \pi$. **(c)** *An eclipse around* $\theta = \frac{3}{2}\pi$.

Figure 3.9: *The reflected light signal* f_B *for eclipses around* $\theta = \frac{\pi}{2}, \pi$ *and* $\frac{3\pi}{2}$. *Each curve has a different shape. The different shapes are explained in the text by the motion of the bodies.*

The shape of the three dips in figure 3.9 are all different. The shape at $\theta = \frac{1}{2}\pi$ occurs at $\theta = \frac{1}{2}\pi$ mod 2π as well, so the shape of the signal depends clearly on the phase. The same goes for the other jumps. The explanation for the effect in figure 3.9 lies in the fact that the planets move counterclockwise.

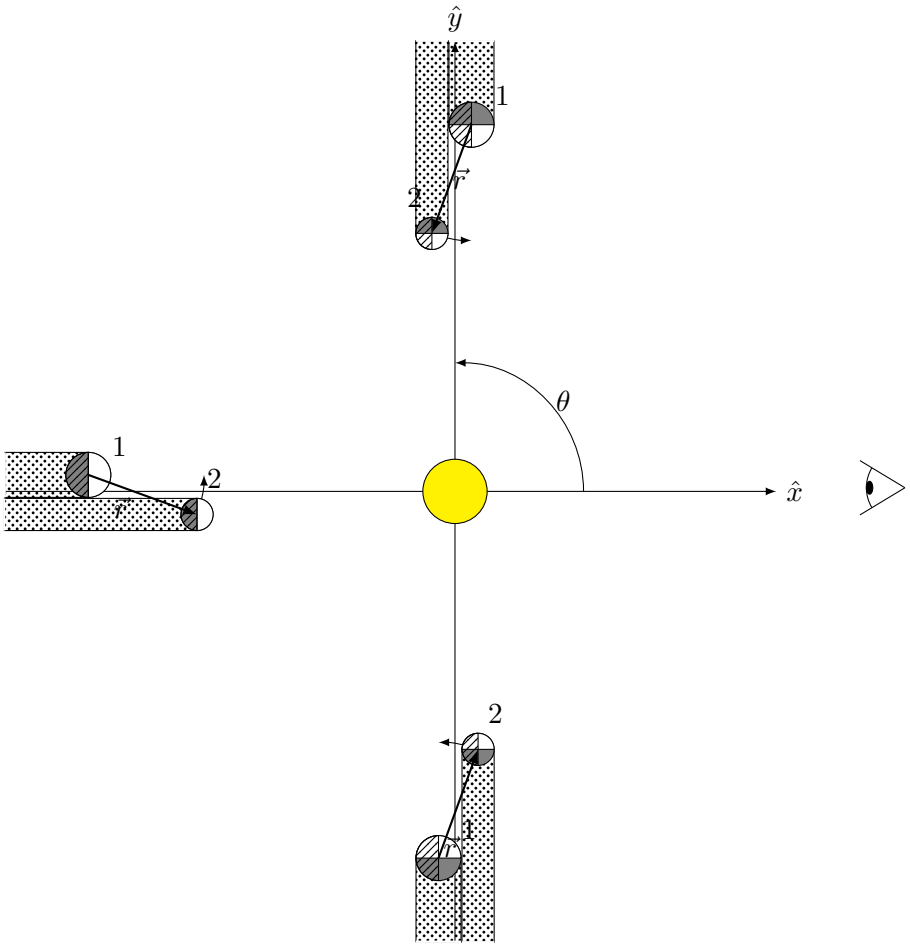

Figure 3.10: *The start of three eclipses at* $\theta = \frac{1}{2}\pi$ *(in positive* $\hat{y}$*-direction),* $\theta = \pi$ *(in negative* $\hat{x}$*-direction) and* $\theta = \frac{3}{2}\pi$ *(in negative* $\hat{y}$*-direction) of the planet by the moon. The dotted area is a shadow cylinder behind the moon with symmetry axis* $\vec{R}(t)$. *The observer is placed in the positive* $\hat{x}$*-direction. The figure is depicted face-on (top-view). The arrows indicate the binary motion. The star is in the origin. The relative vector* $\vec{r}$ *is the vector from the planet to the moon.*

At $\theta = \frac{1}{2}\pi$ first the moon will move in front of the planet at the invisible side of the planet (see figure 3.10). The eclipse only has an influence from the center of cylinder on. The surface region that is dark due to the eclipse is larger in the middle of the cylinder than at the side of the planet. The signal changes are therefore fast. At the end of the eclipse, less surface is dark, namely only the side of the planet. The change in the signal is therefore more gradual. This corresponds to the signal in figure 3.9a. At $\theta = \frac{3}{2}\pi$, the moon will move in front of the planet at the side of the planet that is lit. Here the percentage of the surface area that is dark due to the eclipse is less than the percentage that is dark at the end of the eclipse. The reflected light signal will first decrease slowly. At the end of the eclipse, the reflected light signal will change fast, because it moves away from the middle of the cylinder. At $\theta = \pi$, the situation is symmetric. We expect the signal in figure 3.9b.
For all different phases, it can be verified that the duration of the eclipse equals equation 3.22.

3.7.1 Change planet moon ratio

We compare the total reflected light signal for different values of $\frac{s_1}{s_2}$. We will take values of $s_1 = s_2 = R_{Jup}$, $s_1 = 2s_2 = 2R_{Jup}$, $s_1 = 3s_2 = 3R_{Jup}$ and $s_1 = 10s_2 = 2R_{Jup}$. Large values for the radius of the moon are included, because planet-binary systems and thus large moons may exist [16]. We will plot the reflected light signal f_1, f_2 and f_B all in one figure for every situation, see figure 3.11.

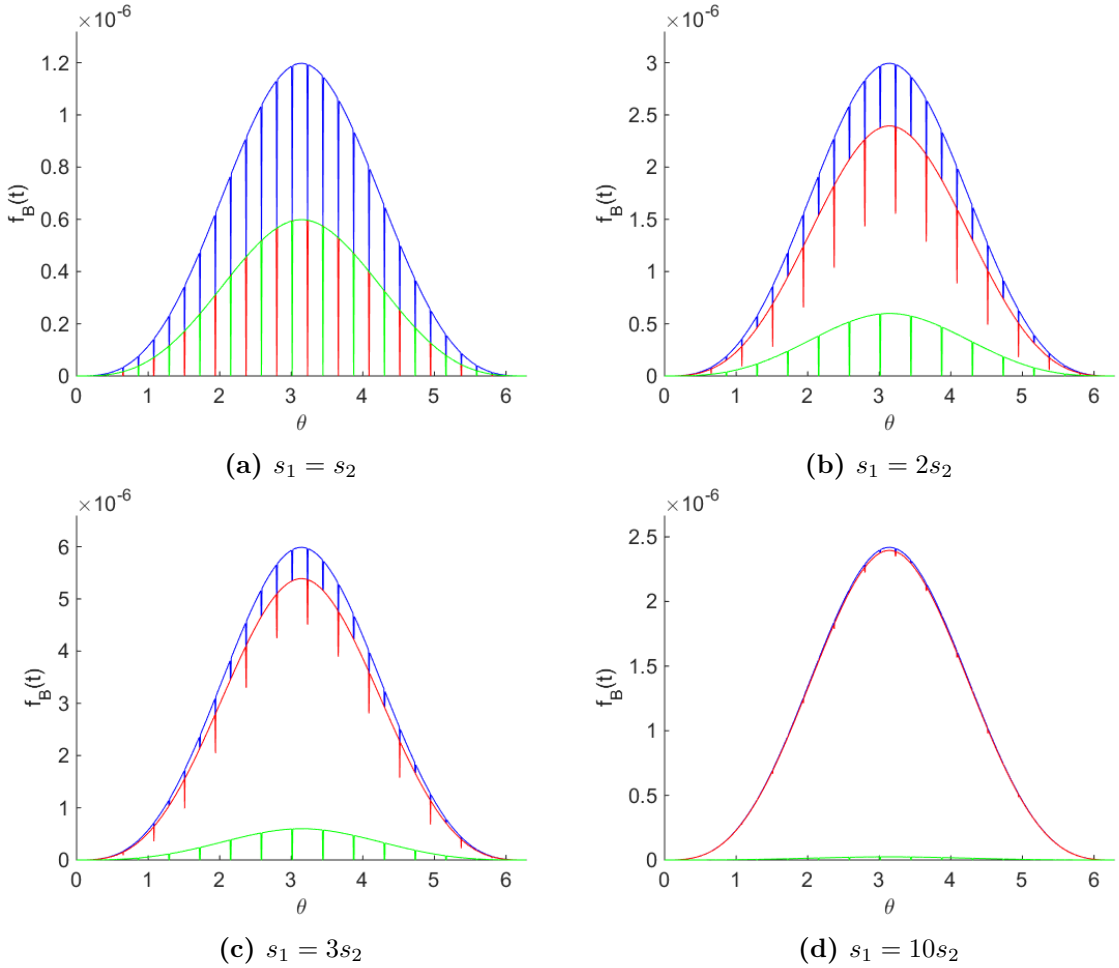

(a) $s_1 = s_2$ **(b)** $s_1 = 2s_2$

(c) $s_1 = 3s_2$ **(d)** $s_1 = 10s_2$

Figure 3.11: *The reflected light signal of f_B in blue, f_1 in red and f_2 in green plotted in one figure against θ. We see different values for $\frac{s_1}{s_2}$ in the subfigures 3.11a, 3.11b, 3.11c and 3.11d.*

In figure 3.11b and 3.11c, the signal f_1 is larger than signal f_2. This is due to the difference in planet radii. Also f_1 has jumps that do not go to zero, while the jumps of f_2 do go to zero. The planet is never completely darkened by the moon. The moon can darken the surface area with a circle with radius s_2. s_1 is larger than s_2, so the circle will never cover the entire planet.

The amount of eclipses does not change for the different situations.
For situation $s_1 = 10s_2$ in figure 3.11d, we almost do not see the jumps anymore. The contribution of the eclipses is almost negligible. With an even larger ratio, the dips indicating eclipses will not be visible anymore.
Astronomers will only see the reflected light signal f_B (blue curve). If astronomers see a signal like in figure 3.11, they would know that there is a chance of an eclipse. They see a quasi-periodic signal that could be explained by a moon.

4 Fourier spectra

In this section the Fourier spectra of the reflected light signals in section 2 and section 3 are derived. The FFT, the fast or discrete Fourier transform, of MATLAB is used. Whether it is a fast or discrete Fourier transform, depends on the number of points that is used.

4.1 Fourier transform of the reflected light signals

The complex Fourier series of a function that is periodic in $\theta \mod 2\pi$ is defined as

$$f(\theta) = \sum_{n=-\infty}^{\infty} f_n e^{i\theta n} \tag{4.1}$$

We define the Fourier transform of the signal the following way

$$\hat{f}(\nu) = \frac{1}{2\pi} \int_{-\infty}^{\infty} f(t) e^{-i\nu t} dt \tag{4.2}$$

and the inverse Fourier transform

$$f(t) = \int_{-\infty}^{\infty} \hat{f}(\nu) e^{i\nu t} d\nu \tag{4.3}$$

For a system with one planet described in paragraph 2.1, f is periodic in $\theta \mod 2\pi$. The Fourier transform is

$$\hat{f}(\nu) = \frac{1}{2\pi} \sum_{n=-\infty}^{\infty} f_n \int_{-\infty}^{\infty} e^{i(n\omega t - \nu t)} dt = \frac{1}{2\pi} \sum_{n=-\infty}^{\infty} f_n 2\pi\delta(\nu - n\omega) = \sum_{n=-\infty}^{\infty} f_n \delta(\nu - n\omega) \tag{4.4}$$

so the Fourier transform of a light curve from one planet is a series of equidistant δ-peaks.
For a system with a planet-binary described in paragraph 3.1, f is determined by configuration of two planets, namely $f = f_1 + f_2$. If the orbital angle of f_1 and f_2 are θ and ϕ respectively, then we deduce from this that $f(t) = f(\theta, \phi)$, where $\theta = \omega t$ and $\phi = \Omega t$. f is a periodic function in $\theta \mod 2\pi$, so $f(\theta + 2\pi, \phi) = f(\theta, \phi)$. f is also a periodic function in $\phi \mod 2\pi$, so $f(\theta, \phi + 2\pi) = f(\theta, \phi)$, and combining this with equation 4.1 gives equation 4.5:

$$f(\theta, \phi) = \sum_{n=-\infty}^{\infty} f_n(\phi) e^{in\theta} \tag{4.5}$$

Because $f(\theta, \phi)$ is periodic in $\phi \mod 2\pi$, so is $f_n(\phi)$. We have $f_n(\phi + 2\pi) = f_n(\phi)$. Thus we have, using a complex Fourier series in equation 4.1,

$$f_n(\phi) = \sum_{m=-\infty}^{\infty} f_n^m e^{im\phi} \tag{4.6}$$

Combining equation 4.5 and 4.6, we get

$$f(t) = f(\theta(t), \phi(t)) = \sum_{n=-\infty}^{\infty} \sum_{m=-\infty}^{\infty} f_n^m e^{in\theta} e^{im\phi} \tag{4.7}$$

If we apply equation 4.7 to the situation where $\theta(t) = \omega t$ and $\phi(t) = \Omega t$, then equation 4.7 will change in equation 4.8:

$$f(t) = f(\omega t, \Omega t) = \sum_{n=-\infty}^{\infty} \sum_{m=-\infty}^{\infty} f_n^m e^{i(n\omega + m\Omega)t} \tag{4.8}$$

So $f(t)$ can be written as a quasiperiodic function with double Fourier series. The Fourier transform (4.2) of equation 4.8 is

$$\hat{f}(\nu) = \sum_{n,m} f_n^m \delta(\nu - n\omega - m\Omega) = \sum_{n,m} f_n^m \delta(n\omega + m\Omega - \nu) \tag{4.9}$$

We look at the Fourier Transform $\hat{f}(\nu + \Omega - \omega)$ at a shifted frequency.

$$\hat{f}(\nu + \Omega - \omega) = \sum_{n,m} f_n^m \delta(-\Omega + \omega + n\omega + m\Omega - \nu) = \sum_{n,m} f_n^m \delta\big((n+1)\omega + (m-1)\Omega - \nu\big) \tag{4.10}$$

$$= \sum_{n,m} f_{n-1}^{m+1} \delta(n\omega + m\Omega - \nu) \tag{4.11}$$

This means that shifting the frequency by $\Omega - \omega$ is a shift in coefficients, $m \to m+1, n \to n-1$.

4.2 Fourier spectra of the light signals

The Fourier spectrum of the reflected light signal in figure 2.7 for a system with one planet is given in figure 4.1.

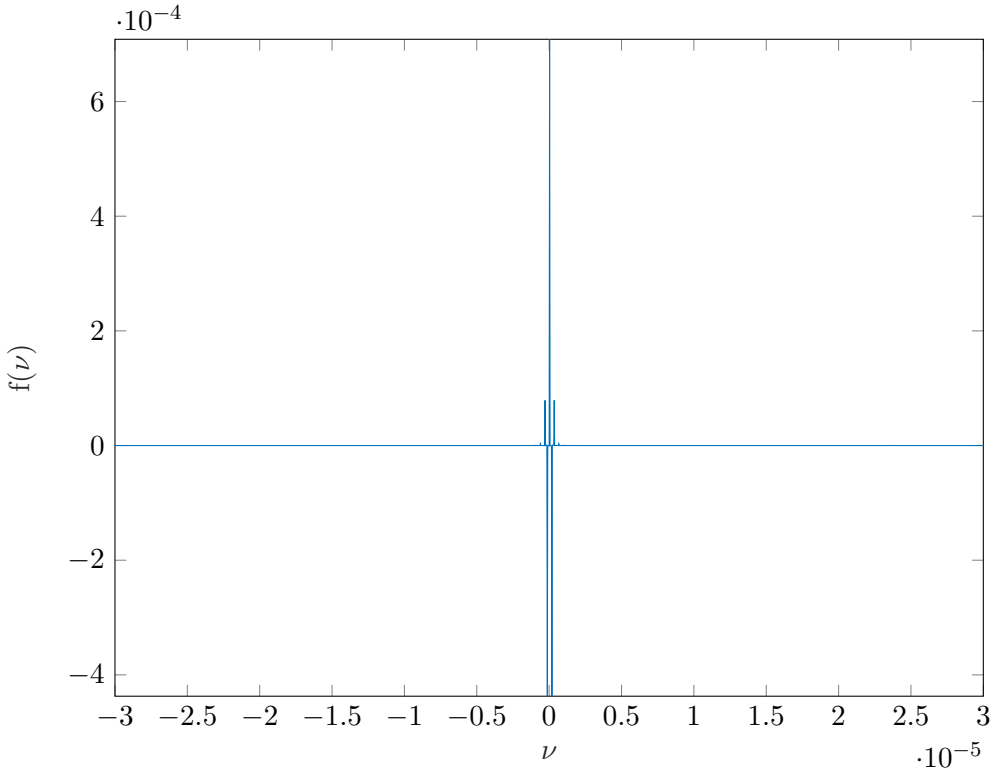

Figure 4.1: *The Fourier spectrum of the reflected light signal of a system with one planet in figure 2.7 in section 2.4. The spectrum is made up of only a few δ-peaks at very low frequencies $\nu = n\omega$.*

In figure 4.2, we zoom in on the δ-peaks at very low frequencies. The Fourier spectrum is symmetric around 0. We recognize 5 different δ-peaks in the Fourier spectrum in figure 4.2. The one closest to 0 is a high peak with height $f_0 > 0$. The second one is a high peak with height $f_1 < 0$. The last one is little peak with height $f_2 > 0$.
In figure 4.3 the Fourier spectrum of the total reflected light signal of a system with a planet-binary described in paragraph 3.1 in figure 3.8 is plotted.

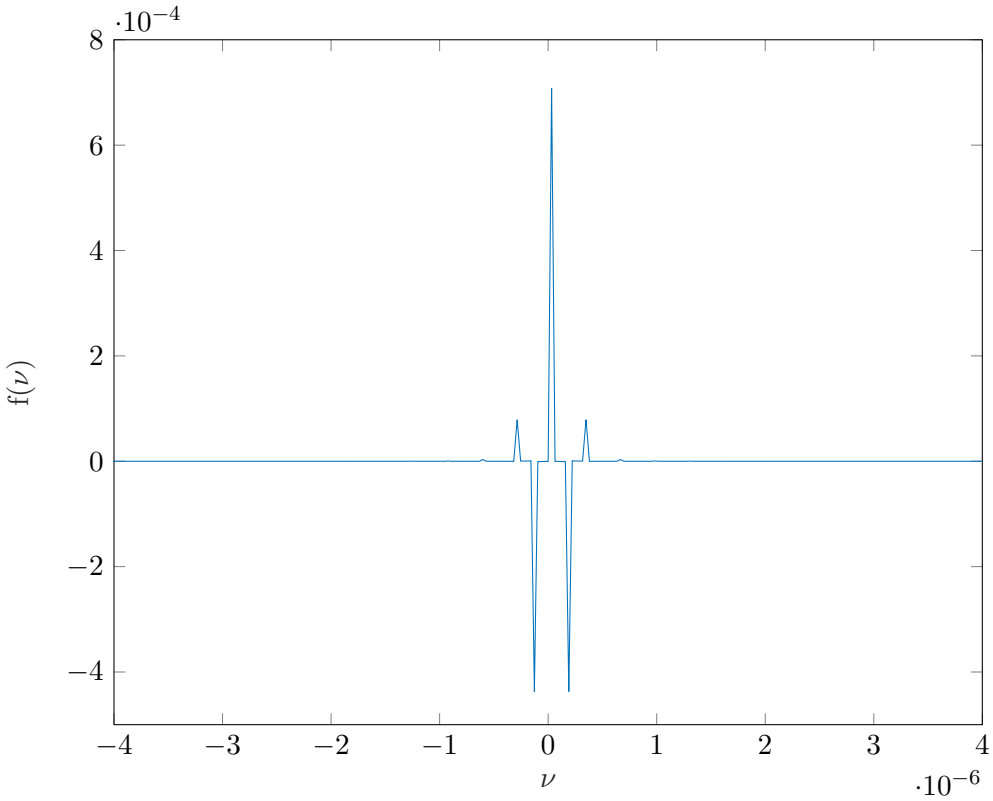

Figure 4.2: *A zoomed in version of the Fourier spectrum of the reflected light signal in figure 4.1. Five peaks are clearly visible. The spectrum is symmetric. The first peak around $\nu = 0$ has strength f_0, the second around $\nu = \omega$ has strength f_1 and the third around $\nu = 2\omega$ has strength f_2.*

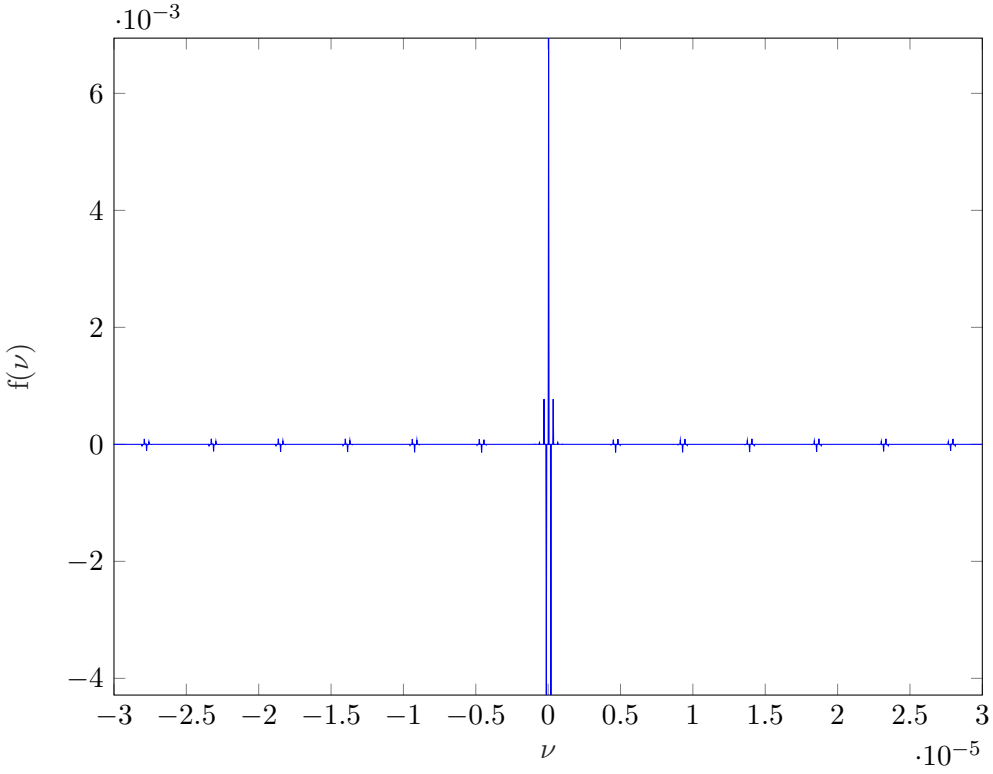

Figure 4.3: *The Fourier spectrum of the total reflected light signal in figure 3.8 for a system with a planet-binary. The Fourier spectrum is almost the same as the spectrum of a system with one planet in figure 4.1. The difference are the little disturbances at higher frequencies $\nu = m\Omega$. These are caused by eclipses.*

Notice that the spectrum in figure 4.1 and in figure 4.3 are much alike. There are small periodic peaks in the spectrum in figure 4.3. These peaks zoomed in are seen in the signal in figure 4.4.

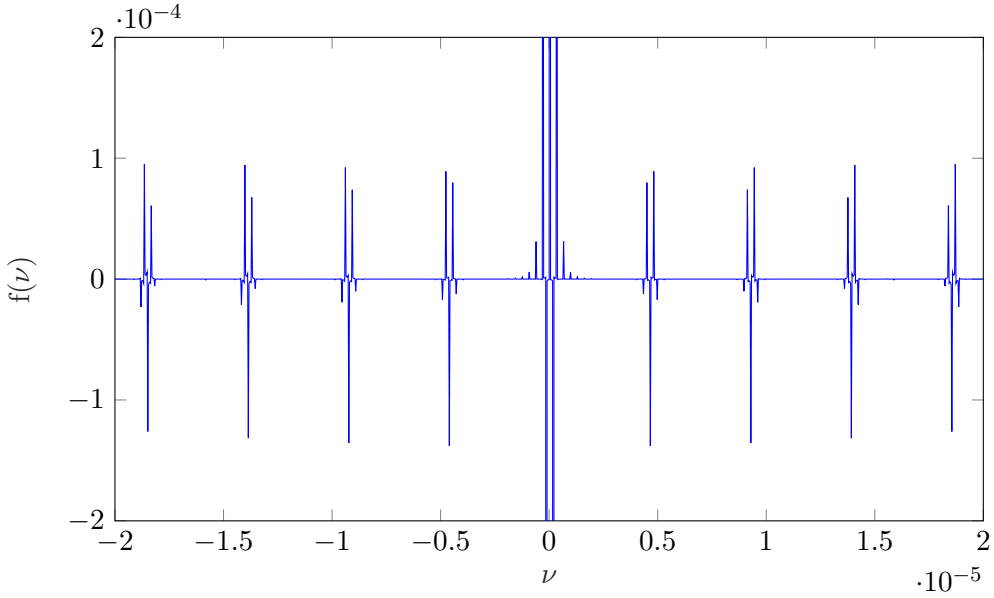

Figure 4.4: *The signal in figure 4.3 zoomed in. The structures at the side are nearly identical.*

If we zoom in on the Fourier spectra of the reflected light signal over only the planet and the moon in figure 3.7, we get figure 4.5 and figure 4.6 respectively.

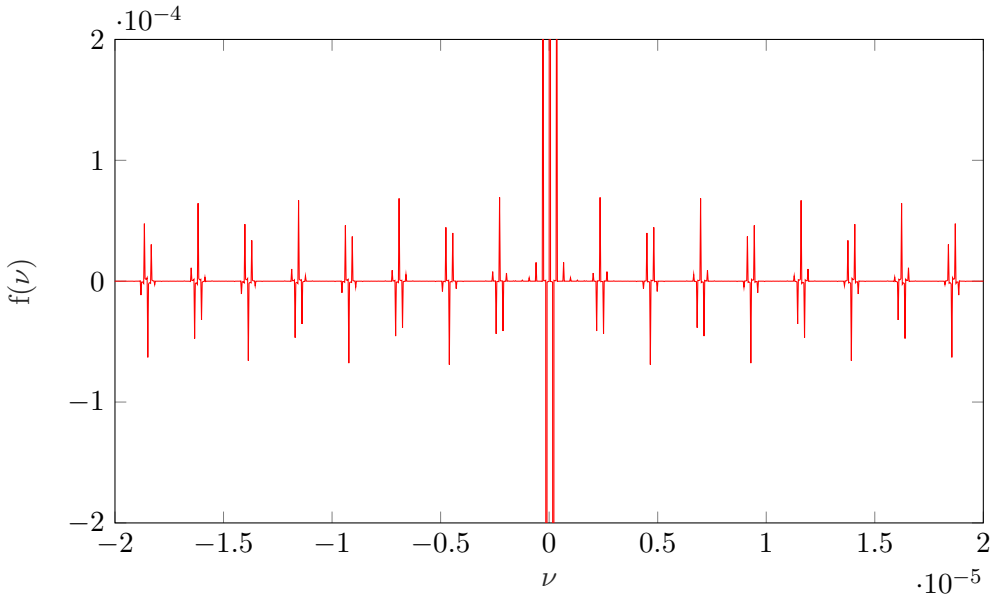

Figure 4.5: *The Fourier spectrum of the reflected light signal from the planet. The side structures are alternatingly flipped in the ν-axis due to eclipses at $\tilde{t}_n$.*

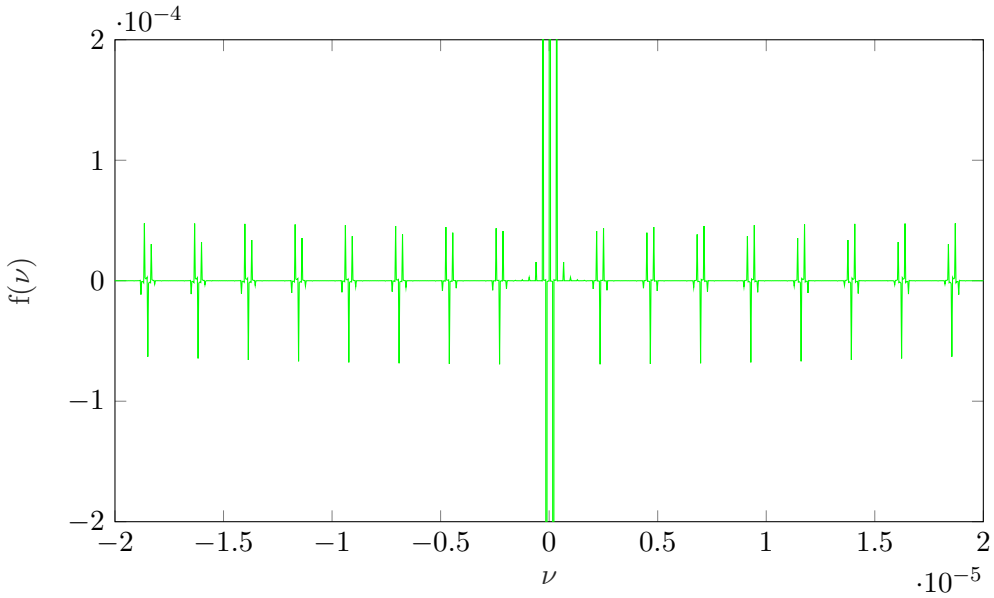

Figure 4.6: *The Fourier spectrum of the reflected light signal from the moon. The side structures are all almost equal due to eclipses at t_n.*

The Fourier spectra of the nett signal of the planet and moon is exactly the Fourier spectrum of the total reflected light signal. The peaks in the Fourier spectra in figure 4.5 and figure 4.6 appear twice as often as in the spectrum of the total reflected signal in figure 4.4. The spectrum of the light signal of the planet has peaks that are each time mirrored in the ν-axis per peak. This is why in the spectrum of the total light signal the peaks appear half as many times as in the spectrum in figure 4.5 or 4.6. The mirrored peaks of the signal in figure 4.5 cancel the peaks of the signal in figure 4.6. The peaks are mirrored due to the initial conditions 3.9 and 3.10. At $t = 0$, the planet is in between the moon and the star. An eclipse occurs at the surface of the moon. This makes the reflected light signal of the moon an even signal and that is why the peaks are all the same.

4.3 Analysis of the Fourier spectra

We can split $f(t)$ in two parts: a part that is due to only the phases of the year $f_D(t)$ and a part that is due to the eclipses $f_E(t)$.

$$f(t) = f_D(t) + f_E(t) \tag{4.12}$$

Notice that $f(t), f_D(t) \geq 0$ and that $f_E \leq 0$. $f_D(t)$ is periodic modulo $\frac{2\pi}{\omega}$. In figure 3.9 we can see that the peaks of the eclipses have a very short duration. We can approximate the short peaks with delta peaks at the times of the total eclipses $t_n = \frac{\pi n}{\Omega - \omega}$. So then

$$f_E(t) = \sum_{n=-\infty}^{\infty} g_n \delta(t - t_n) \tag{4.13}$$

with $g_n \leq 0$. The Fourier transform 4.2 of this signal is

$$f_E(\nu) = \frac{1}{2\pi} \sum_{n=-\infty}^{\infty} g_n e^{-i\nu t_n} \tag{4.14}$$

We compute the Fourier transform of $f_E(\nu + \Omega - \omega)$, combine that with $t_n = \frac{\pi n}{\Omega - \omega}$. We get

$$f_E(\nu + \Omega - \omega) = \frac{1}{2\pi} \sum_{n=-\infty}^{\infty} g_n e^{-i(\nu + \Omega - \omega)t_n} = \frac{1}{2\pi} \sum_{n=-\infty}^{\infty} g_n e^{-i\nu t_n - i(\Omega - \omega)\frac{\pi n}{\Omega - \omega}} = \pm \frac{1}{2\pi} \sum_{n=-\infty}^{\infty} g_n e^{-i\nu t_n} \tag{4.15}$$

Notice that for even n

$$f_E(\nu) = f_E(\nu + \Omega - \omega) \tag{4.16}$$

so the Fourier transform of $f_E(t)$ is periodic with period $\Omega - \omega$. If from equation 4.9 and equation 4.10, we only assume the part that is due to the eclipses and fill this in in equation 4.16, we get:

$$f_E(\nu) = \sum_{n,m} (f_E)_n^m \delta(n\omega + m\Omega - \nu) = \sum_{n,m} (f_E)_{n-1}^{m+1} \delta(n\omega + m\Omega - \nu) = f_E(\nu + \Omega - \omega) \tag{4.17}$$

and therefore we get

$$(f_E)_n^m = (f_E)_{n-1}^{m+1} \forall n, m \in \mathbb{Z} \tag{4.18}$$

Because this holds $\forall n, m \in \mathbb{Z}$,

$$(f_E)_n^m = (f_E)_{n-k}^{m+k} \forall n, m, k \in \mathbb{Z} \tag{4.19}$$

and with $k = -m$

$$(f_E)_n^m = (f_E)_{n+m}^0 \tag{4.20}$$

From equation 4.20, we see that the peaks will repeat themselves. This is also what is noticed in figures 4.2, 4.3, 4.5 and 4.6.

5 Inclination of binary plane

A moon does not always orbit around the planet in the same plane as the planet around the star, see table 2. For example, our own Moon has a tilt in its orbit of around 5 degrees. The Pluto/Charon system has an even larger angle of 118 degrees. The tilt in the orbit of the moon with respect to the orbit of the planet we will call inclination. For this reason we also consider inclination in this thesis.

System	s_1 [km]	s_2 [km]	r [km]	α [°]	α^* [-]	ω [rad/year]	Ω [rad/day]
Earth/Moon	6371.0	1737.1	384400	5.145	4.25	2π	0.22997
Pluto/Charon	1186 ± 2	604 ± 1.5	19570	118	9.6	0.0253	0.9837
Saturn/Titan	58232	2575 ± 2	1221870	26.7	9.0	0.213	0.394

Table 2: *Radii, distance, inclination and orbital frequencies of the Earth/Moon, Pluto/Charon and Saturn/Titan system. The values are found (or calculated by using values) at [12], [17], [18], [19], [20], [21], [22] and [23].*

5.1 Theory of inclination

The plane in which the planet and the moon orbit each other, can be rotated with an angle α around the x-axis, see figure 5.1.

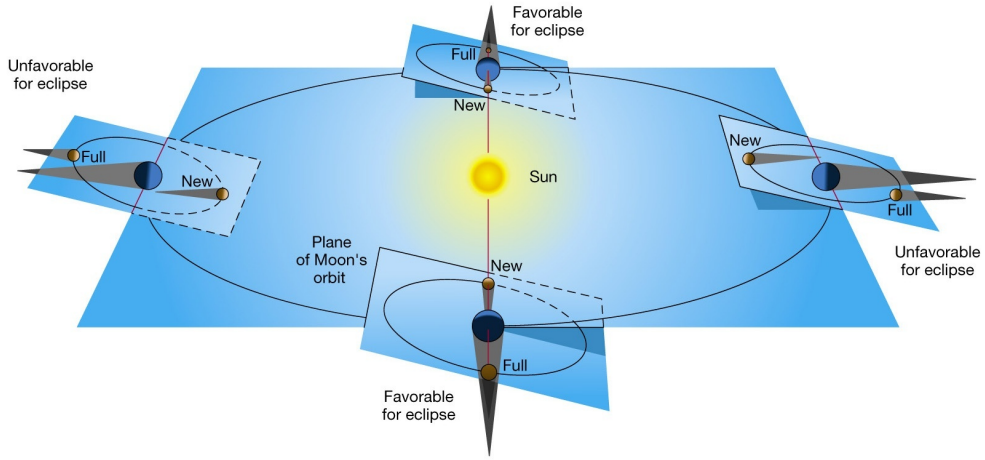

Figure 5.1: *Inclination of the plane of the orbit of the Moon with respect to the orbit of the Earth [24]. The tilt of the plane is called the inclination α. The Moon is aligned with the Earth and the Sun two times a year (in two not successive seasons). An eclipse can occur at that time. In the other seasons, the Moon, the Sun and the Earth can only be aligned if the tilt is very small.*

This happens when $\vec{r}$ is multiplied by the rotational matrix from [13]:

$$\mathcal{A} = \begin{pmatrix} 1 & 0 & 0 \\ 0 & \cos(\alpha) & -\sin(\alpha) \\ 0 & \sin(\alpha) & \cos(\alpha) \end{pmatrix} \tag{5.1}$$

then

$$\mathcal{A}\vec{r} = r \begin{pmatrix} 1 & 0 & 0 \\ 0 & \cos(\alpha) & -\sin(\alpha) \\ 0 & \sin(\alpha) & \cos(\alpha) \end{pmatrix} \begin{pmatrix} \cos(\Omega t) \\ \sin(\Omega t) \\ 0 \end{pmatrix} = r \begin{pmatrix} \cos(\Omega t) \\ \cos(\alpha)\sin(\Omega t) \\ \sin(\alpha)\sin(\Omega t) \end{pmatrix} \tag{5.2}$$

In this case we have for the positioning of the planet and the moon

$$\vec{R}_1(t) = R \begin{pmatrix} \cos(\omega t) \\ \sin(\omega t) \\ 0 \end{pmatrix} - \frac{m_2 r}{m_1 + m_2} \begin{pmatrix} \cos(\Omega t) \\ \cos(\alpha)\sin(\Omega t) \\ \sin(\alpha)\sin(\Omega t) \end{pmatrix} \tag{5.3}$$

$$\vec{R}_2(t) = R \begin{pmatrix} \cos(\omega t) \\ \sin(\omega t) \\ 0 \end{pmatrix} + \frac{m_1 r}{m_1 + m_2} \begin{pmatrix} \cos(\Omega t) \\ \cos(\alpha)\sin(\Omega t) \\ \sin(\alpha)\sin(\Omega t) \end{pmatrix} \tag{5.4}$$

Note that the node of the inclined plane is the x-axis. The initial situation (at $t = 0$) will still be the same as with the situation without the inclination 3.9 and 3.10. Notice that if $\alpha = 0$, equation 5.3 and 5.4 reduce to equation 3.7 and 3.8, the situation of zero inclination.

5.2 Effective inclination value

When projected on the plane perpendicular to $\hat{R}$, there is a displacement l in the motion of the center of the moon with respect to the center of the planet. If $\alpha = 0$, then $l = 0$. If $\alpha \neq 0$, then l could be larger than 0. The duration of an eclipse is derived in paragraph 3.4 and is given in equation 3.22. The duration of an eclipse in an inclined plane is always smaller or equal to that value of equation 3.22. This is explained by the displacement l in figure 5.2. If there is a displacement $l > 0$, the moon is in between the star and the planet for a shorter period of time. The moon passes the planet faster.

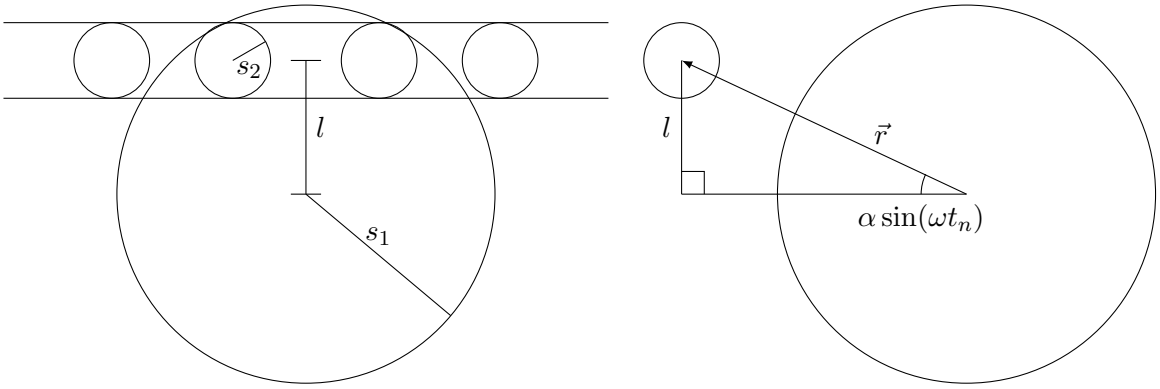

(a) *View from star.* **(b)** *View rotated with $\frac{\pi}{2}$ around the z-axis.*

Figure 5.2: *An eclipse on the planet by the moon. In figure 5.2a, the view is from the star. In figure 5.2a, the view is rotated by $\frac{\pi}{2}$ around the z-axis. l is the displacement of the motion of the center of the moon with respect to the center of the planet. At $\alpha = 0$, $l = 0$.*

The shadow displacement l is

$$l = \alpha r \sin(\omega t_n) \tag{5.5}$$

The maximum value for l is

$$l_{max} = \alpha r \tag{5.6}$$

The value for l_{max} where just an eclipse can be seen is $s_1 + s_2$. We define the effective inclination value α^* as

$$\alpha^* = \frac{l_{max}}{s_1 + s_2} = \frac{\alpha r}{s_1 + s_2} \tag{5.7}$$

For an eclipse to be seen at l_{max}, $\alpha^* \leq 1$.

5.3 Changing effective inclination value

We will study different values of α^*. The values for α^* will be 0, $\frac{1}{2}$, 1 and $\frac{3}{2}$. We as well will vary $\frac{s_1}{s_2}$ with values 1, 2, 3 and 10. The results are in figure 5.3.

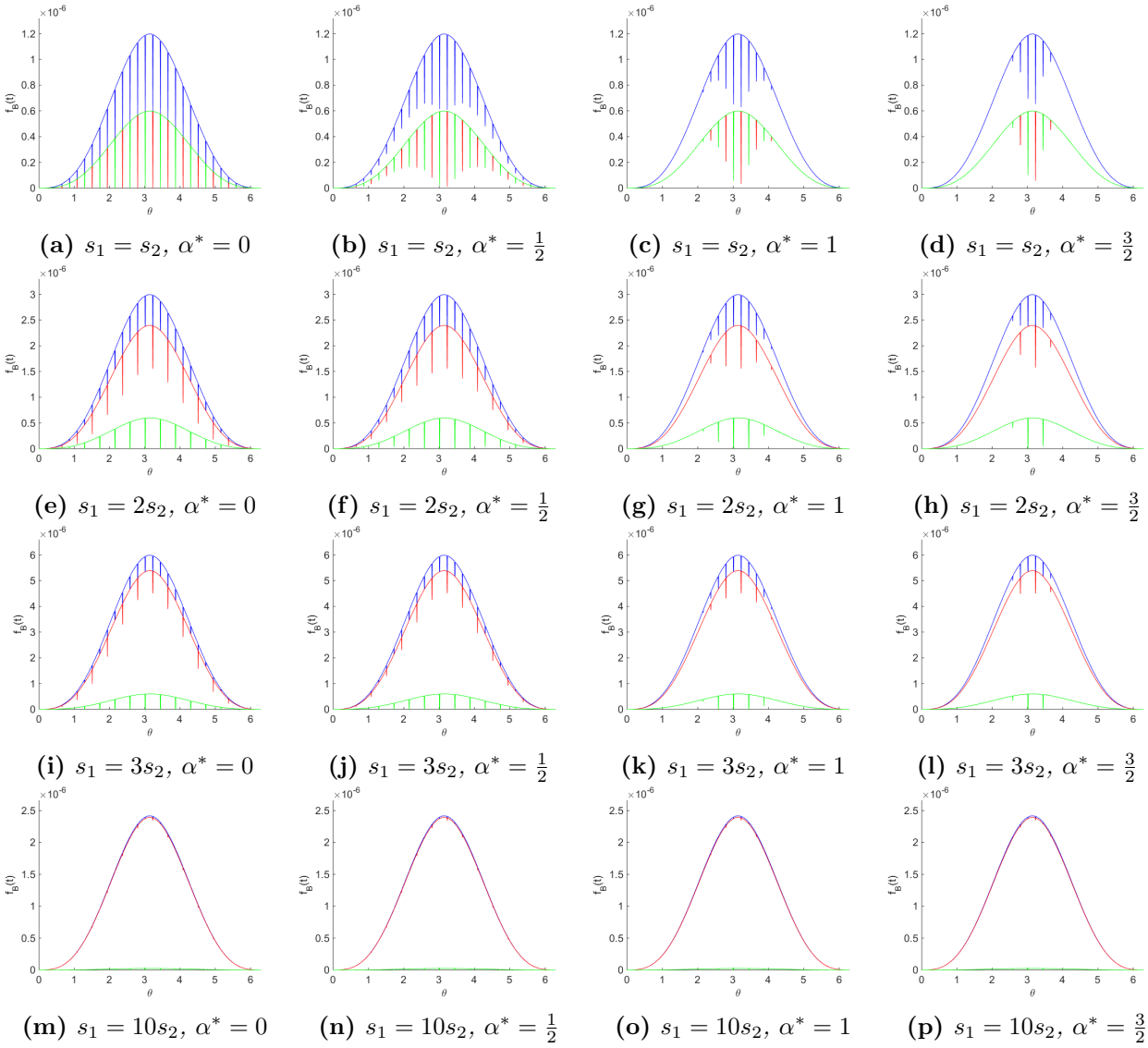

(a) $s_1 = s_2,\ \alpha^* = 0$ **(b)** $s_1 = s_2,\ \alpha^* = \frac{1}{2}$ **(c)** $s_1 = s_2,\ \alpha^* = 1$ **(d)** $s_1 = s_2,\ \alpha^* = \frac{3}{2}$

(e) $s_1 = 2s_2,\ \alpha^* = 0$ **(f)** $s_1 = 2s_2,\ \alpha^* = \frac{1}{2}$ **(g)** $s_1 = 2s_2,\ \alpha^* = 1$ **(h)** $s_1 = 2s_2,\ \alpha^* = \frac{3}{2}$

(i) $s_1 = 3s_2,\ \alpha^* = 0$ **(j)** $s_1 = 3s_2,\ \alpha^* = \frac{1}{2}$ **(k)** $s_1 = 3s_2,\ \alpha^* = 1$ **(l)** $s_1 = 3s_2,\ \alpha^* = \frac{3}{2}$

(m) $s_1 = 10s_2,\ \alpha^* = 0$ **(n)** $s_1 = 10s_2,\ \alpha^* = \frac{1}{2}$ **(o)** $s_1 = 10s_2,\ \alpha^* = 1$ **(p)** $s_1 = 10s_2,\ \alpha^* = \frac{3}{2}$

Figure 5.3: *Reflected light signals for different inclination values and different radii. From left to right, the inclination value a^* takes on values 0, $\frac{1}{2}$, 1 and $\frac{3}{2}$. From top to bottom, the value $\frac{s_1}{s_2}$ takes on values 1, 2, 3, and 10. The red curve is the reflected light signal over the planet f_1, the green curve over the moon f_2 and the blue curve is the total reflected light signal f_B of the bodies.*

Notice the figures in the first row in figure 5.3. When $\alpha^* = \frac{1}{2}$, the eclipse peaks will not go to zero anymore. Due to the inclination, the bodies do not completely block each other. We only see eclipses around $\theta = \pi$, when α^* becomes larger. The inclination angle is too large to form eclipses when the lift $l = l_{max}$. The peaks seen are the eclipses formed at the intersection line of the plane in which the barycenter orbits the star and the plane in which the two bodies orbit. This intersection line is then aligned with r, the vector between the two bodies. In the second and third row we see the same happening, but with smaller peaks. In the last row we almost see no differences between the light signals in the different figures.
The Fourier spectrum of each total reflected light signal is plotted in figure 5.4.

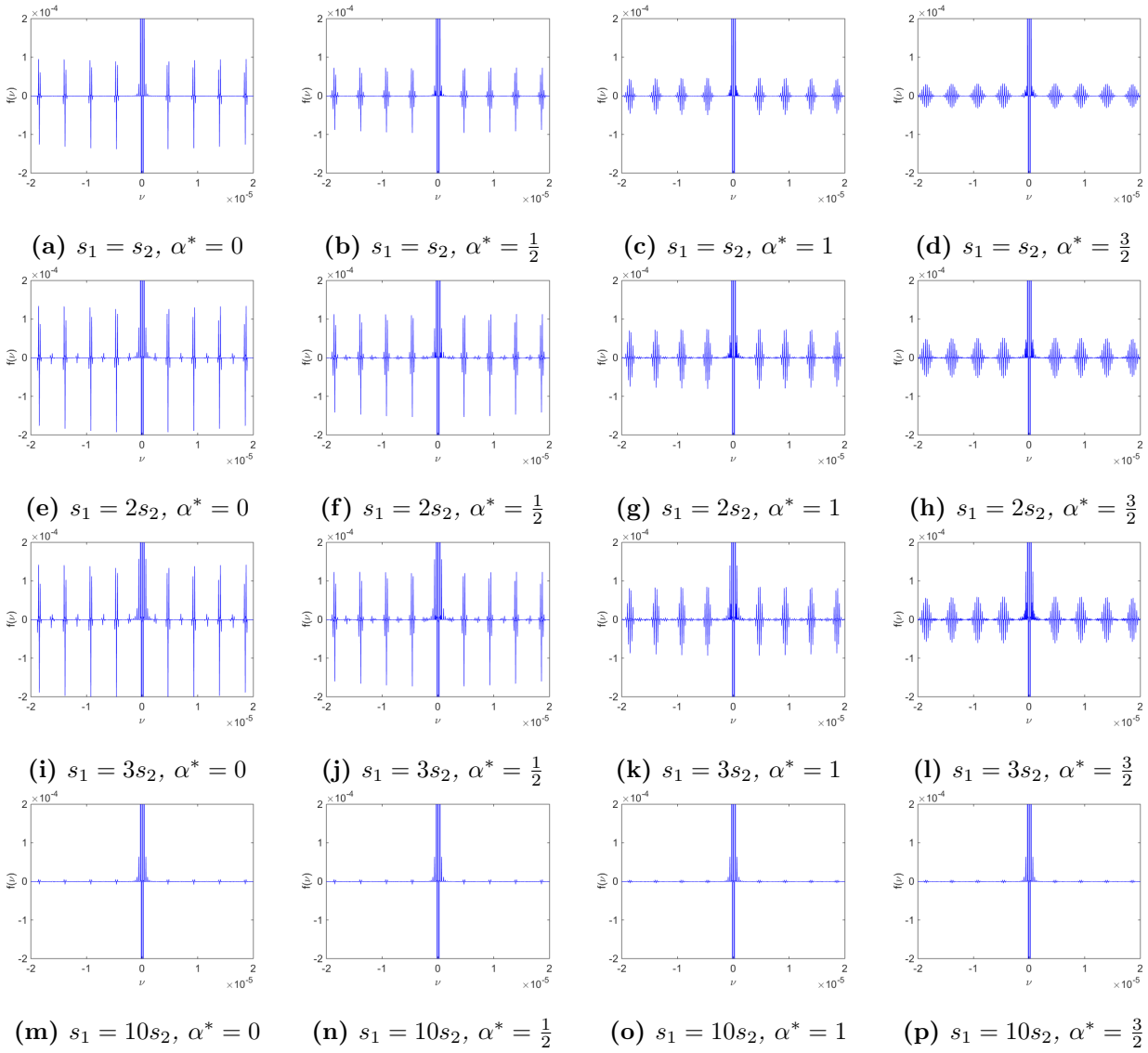

(a) $s_1 = s_2$, $\alpha^* = 0$ **(b)** $s_1 = s_2$, $\alpha^* = \frac{1}{2}$ **(c)** $s_1 = s_2$, $\alpha^* = 1$ **(d)** $s_1 = s_2$, $\alpha^* = \frac{3}{2}$

(e) $s_1 = 2s_2$, $\alpha^* = 0$ **(f)** $s_1 = 2s_2$, $\alpha^* = \frac{1}{2}$ **(g)** $s_1 = 2s_2$, $\alpha^* = 1$ **(h)** $s_1 = 2s_2$, $\alpha^* = \frac{3}{2}$

(i) $s_1 = 3s_2$, $\alpha^* = 0$ **(j)** $s_1 = 3s_2$, $\alpha^* = \frac{1}{2}$ **(k)** $s_1 = 3s_2$, $\alpha^* = 1$ **(l)** $s_1 = 3s_2$, $\alpha^* = \frac{3}{2}$

(m) $s_1 = 10s_2$, $\alpha^* = 0$ **(n)** $s_1 = 10s_2$, $\alpha^* = \frac{1}{2}$ **(o)** $s_1 = 10s_2$, $\alpha^* = 1$ **(p)** $s_1 = 10s_2$, $\alpha^* = \frac{3}{2}$

Figure 5.4: *The Fourier spectra of the reflected light signals seen in figure 5.3. From left to right, the inclination value a^* takes on values 0, $\frac{1}{2}$, 1 and $\frac{3}{2}$. From top to bottom, the value $\frac{s_1}{s_2}$ takes on values 1, 2, 3, and 10. The blue curve is the Fourier transform of the sum of the planets. In every plot, the axes are the same.*

The difference in the Fourier spectra for a binary-planet system with inclination with respect to no inclination is a spreading of the eclipse peaks. The peaks becomes spread out, because the eclipse do not occur with enough periodicity anymore to determine different peaks. In the fourth row, the spectra do not change that much, since the signal is very small.

5.4 Observer in $\hat{y}$ and $\hat{z}$ direction

In this section we will examine the change in the observer's direction to the $\hat{y}$ and $\hat{z}$-direction. The imaginary and the real part of the Fourier transform are plotted. The phase of the Fourier spectra is plotted as well.

5.4.1 $\hat{y}$-direction

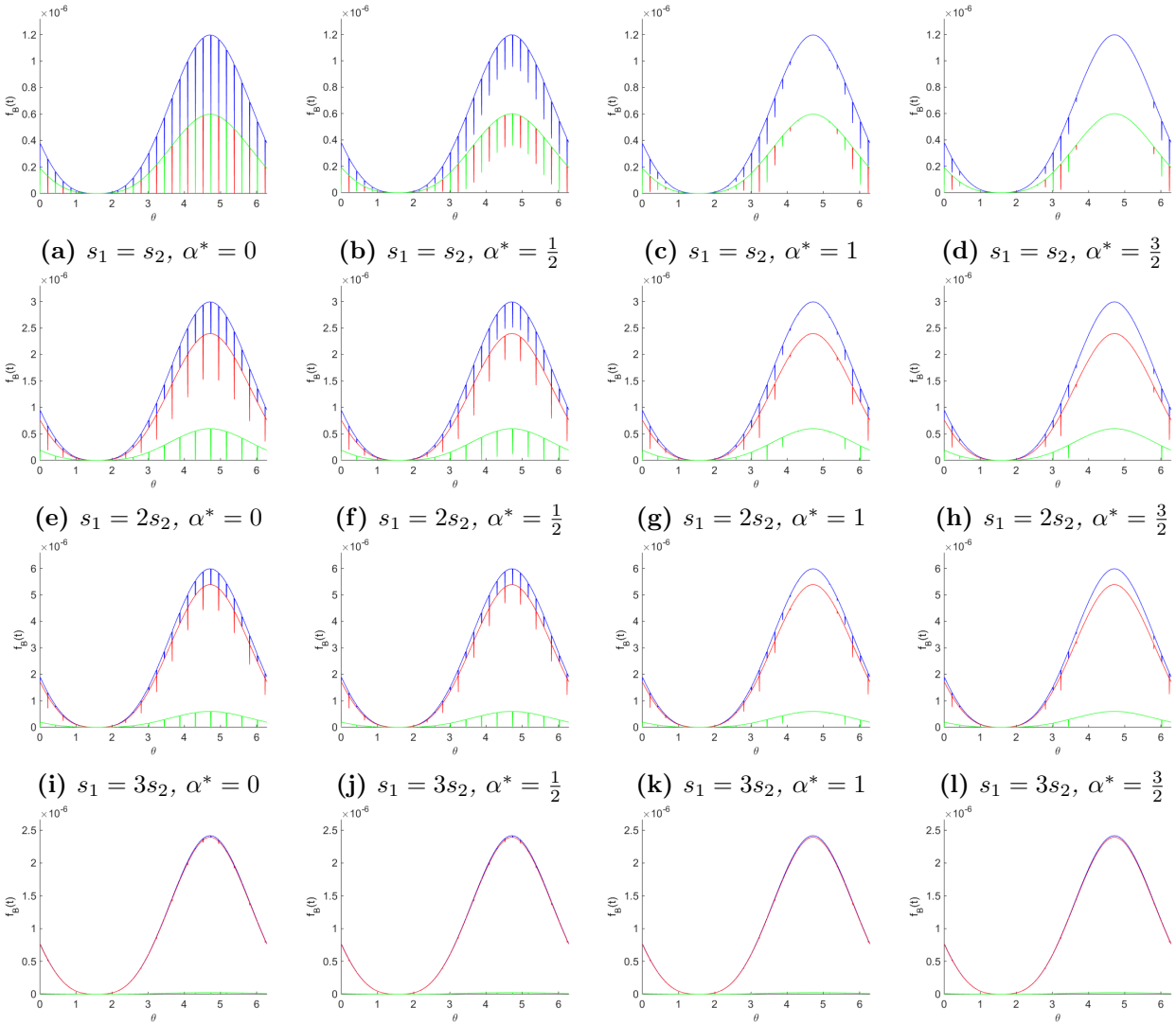

(a) $s_1 = s_2$, $\alpha^* = 0$ **(b)** $s_1 = s_2$, $\alpha^* = \frac{1}{2}$ **(c)** $s_1 = s_2$, $\alpha^* = 1$ **(d)** $s_1 = s_2$, $\alpha^* = \frac{3}{2}$

(e) $s_1 = 2s_2$, $\alpha^* = 0$ **(f)** $s_1 = 2s_2$, $\alpha^* = \frac{1}{2}$ **(g)** $s_1 = 2s_2$, $\alpha^* = 1$ **(h)** $s_1 = 2s_2$, $\alpha^* = \frac{3}{2}$

(i) $s_1 = 3s_2$, $\alpha^* = 0$ **(j)** $s_1 = 3s_2$, $\alpha^* = \frac{1}{2}$ **(k)** $s_1 = 3s_2$, $\alpha^* = 1$ **(l)** $s_1 = 3s_2$, $\alpha^* = \frac{3}{2}$

(m) $s_1 = 10s_2$, $\alpha^* = 0$ **(n)** $s_1 = 10s_2$, $\alpha^* = \frac{1}{2}$ **(o)** $s_1 = 10s_2$, $\alpha^* = 1$ **(p)** $s_1 = 10s_2$, $\alpha^* = \frac{3}{2}$

Figure 5.5: *Reflected light signals for different inclination values and different radii with the observer in the $\hat{y}$-direction. From left to right, the inclination a^* takes on values 0, $\frac{1}{2}$, 1 and $\frac{3}{2}$. From top to bottom, $\frac{s_1}{s_2}$ takes on values 1, 2, 3, and 10. The red curve is the reflected light signal over the planet f_1, the green curve over the moon f_2 and the blue curve is the total reflected light signal f_B of the bodies.*

The reflected light signal of an observer in the $\hat{y}$-direction is plotted in figure 5.5. The shape of the signals differs from the signal of an observer in the $\hat{x}$-direction. This is because the planet and moon have the same initial condition, but the phase at the initial condition changes with the change of observer direction. That is the reason why it is only a phase shift with respect to the $\hat{x}$-direction. We also can see that eclipses are found around $\theta = k\pi \ \forall k \in \mathbb{Z}$ for every inclination angle. This is the same as in the $\hat{x}$-direction, because the intersection line of the two planes is then still aligned with r. In figure 5.6, the real (in blue) and imaginary part (in purple) of the Fourier spectra of the reflected light signals is plotted for every graph in figure 5.5.

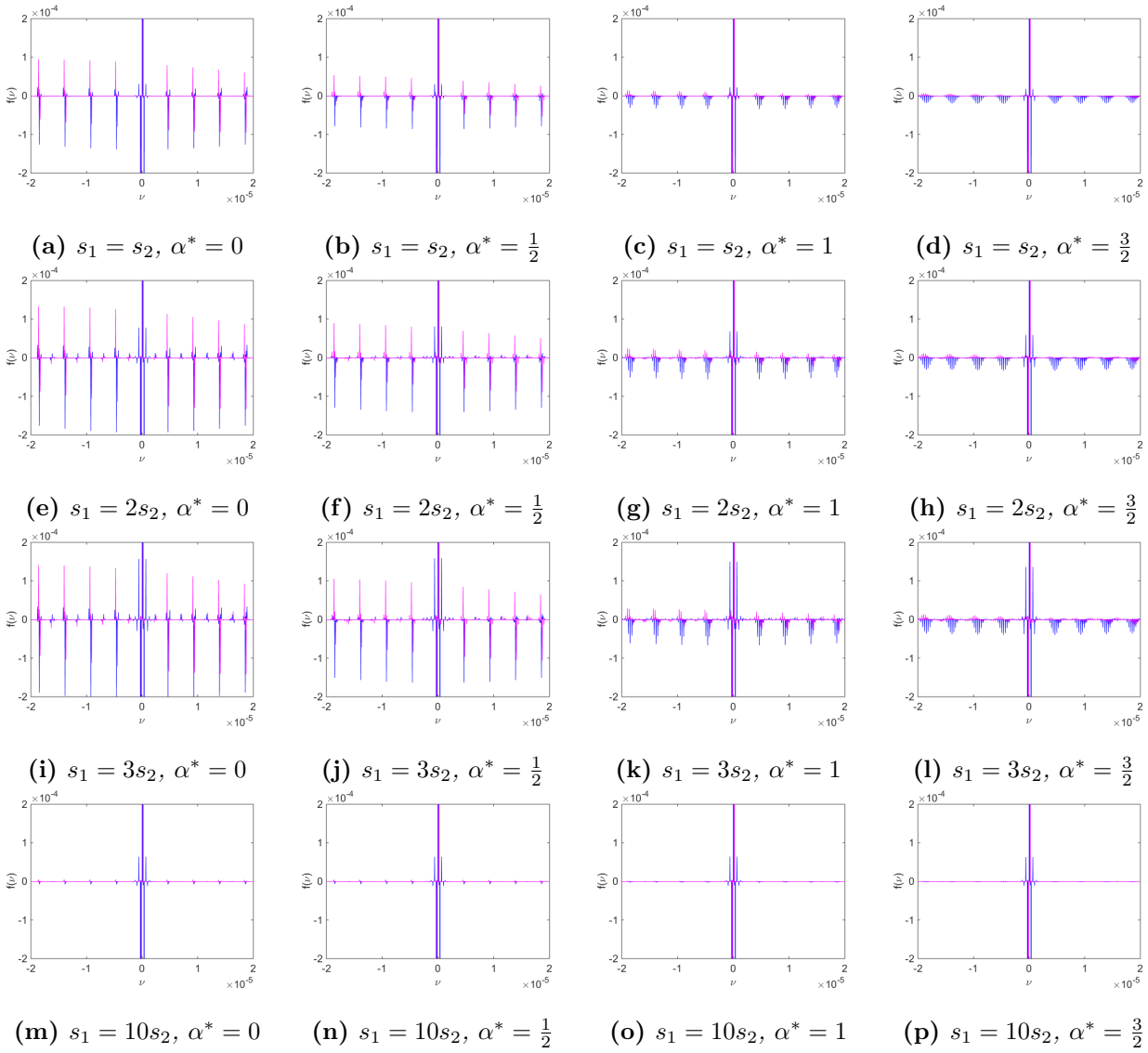

(a) $s_1 = s_2$, $\alpha^* = 0$ **(b)** $s_1 = s_2$, $\alpha^* = \frac{1}{2}$ **(c)** $s_1 = s_2$, $\alpha^* = 1$ **(d)** $s_1 = s_2$, $\alpha^* = \frac{3}{2}$

(e) $s_1 = 2s_2$, $\alpha^* = 0$ **(f)** $s_1 = 2s_2$, $\alpha^* = \frac{1}{2}$ **(g)** $s_1 = 2s_2$, $\alpha^* = 1$ **(h)** $s_1 = 2s_2$, $\alpha^* = \frac{3}{2}$

(i) $s_1 = 3s_2$, $\alpha^* = 0$ **(j)** $s_1 = 3s_2$, $\alpha^* = \frac{1}{2}$ **(k)** $s_1 = 3s_2$, $\alpha^* = 1$ **(l)** $s_1 = 3s_2$, $\alpha^* = \frac{3}{2}$

(m) $s_1 = 10s_2$, $\alpha^* = 0$ **(n)** $s_1 = 10s_2$, $\alpha^* = \frac{1}{2}$ **(o)** $s_1 = 10s_2$, $\alpha^* = 1$ **(p)** $s_1 = 10s_2$, $\alpha^* = \frac{3}{2}$

Figure 5.6: *The Fourier spectra of the reflected light signals seen in figure 5.5 in the $\hat{y}$-direction. The real part of the Fourier spectra is plotted in blue, the imaginary part in purple. From left to right, the inclination a^* takes on values 0, $\frac{1}{2}$, 1 and $\frac{3}{2}$. From top to bottom, the $\frac{s_1}{s_2}$ takes on values 1, 2, 3, and 10. In every plot, the axes are the same.*

In the $\hat{y}$-direction, the reflected light signal is not an even function anymore. This is why an imaginary part of the Fourier spectrum is present. We can still see δ-peaks visible in the spectra. The same goes for the spreading of the spectra when the inclination plays a part.
If an astronomer would see this results, he could think of an exomoon, because the side bands occur with periodicity. But it is not determined yet from these results.
In figure 5.7, the phase of the Fourier spectra of the reflected light signal of the $\hat{y}$-direction is given.

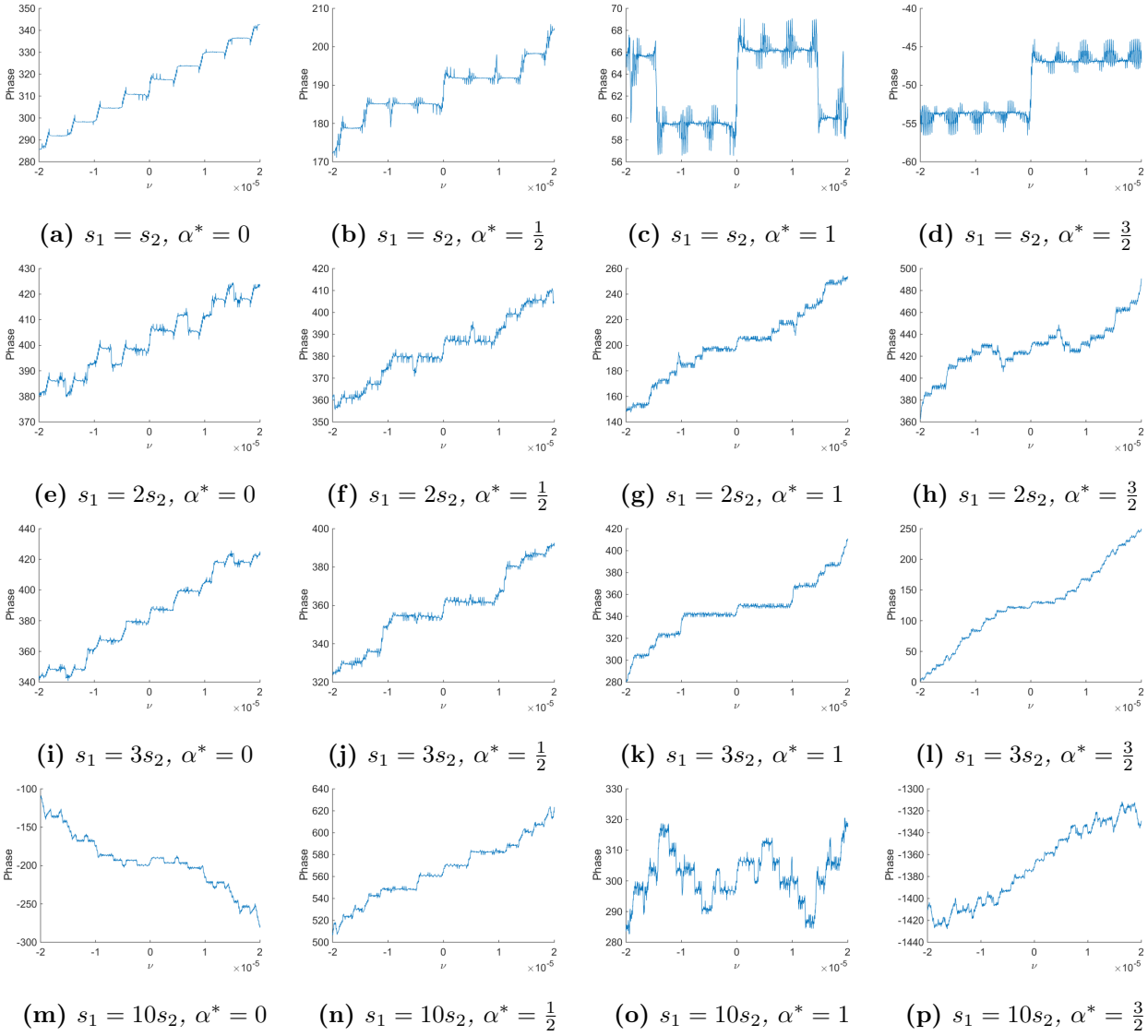

(a) $s_1 = s_2,\ \alpha^* = 0$ **(b)** $s_1 = s_2,\ \alpha^* = \frac{1}{2}$ **(c)** $s_1 = s_2,\ \alpha^* = 1$ **(d)** $s_1 = s_2,\ \alpha^* = \frac{3}{2}$

(e) $s_1 = 2s_2,\ \alpha^* = 0$ **(f)** $s_1 = 2s_2,\ \alpha^* = \frac{1}{2}$ **(g)** $s_1 = 2s_2,\ \alpha^* = 1$ **(h)** $s_1 = 2s_2,\ \alpha^* = \frac{3}{2}$

(i) $s_1 = 3s_2,\ \alpha^* = 0$ **(j)** $s_1 = 3s_2,\ \alpha^* = \frac{1}{2}$ **(k)** $s_1 = 3s_2,\ \alpha^* = 1$ **(l)** $s_1 = 3s_2,\ \alpha^* = \frac{3}{2}$

(m) $s_1 = 10s_2,\ \alpha^* = 0$ **(n)** $s_1 = 10s_2,\ \alpha^* = \frac{1}{2}$ **(o)** $s_1 = 10s_2,\ \alpha^* = 1$ **(p)** $s_1 = 10s_2,\ \alpha^* = \frac{3}{2}$

Figure 5.7: *The phase of the Fourier transform (in radians) of the reflected light signal in the $\hat{y}$-direction. From left to right, the inclination a^* takes on values 0, $\frac{1}{2}$, 1 and $\frac{3}{2}$. From top to bottom, the $\frac{s_1}{s_2}$ takes on values 1, 2, 3, and 10. The real and imaginary part of the Fourier spectra were plotted in figure 5.6.*

5.4.2 $\hat{z}$-direction

In this section, the observer's direction is changed to the $\hat{z}$-direction. In figure 5.8, the reflected light signal is plotted. We now see a totally different signal than in the $\hat{x}$ or $\hat{y}$-direction, because the system is not edge-on anymore. The system is face-on here. A face-on system gives a constant signal, because each position of the planets will give the phase half moon. But still, eclipses occur with some periodicity, which result in dips in the reflected light signal.

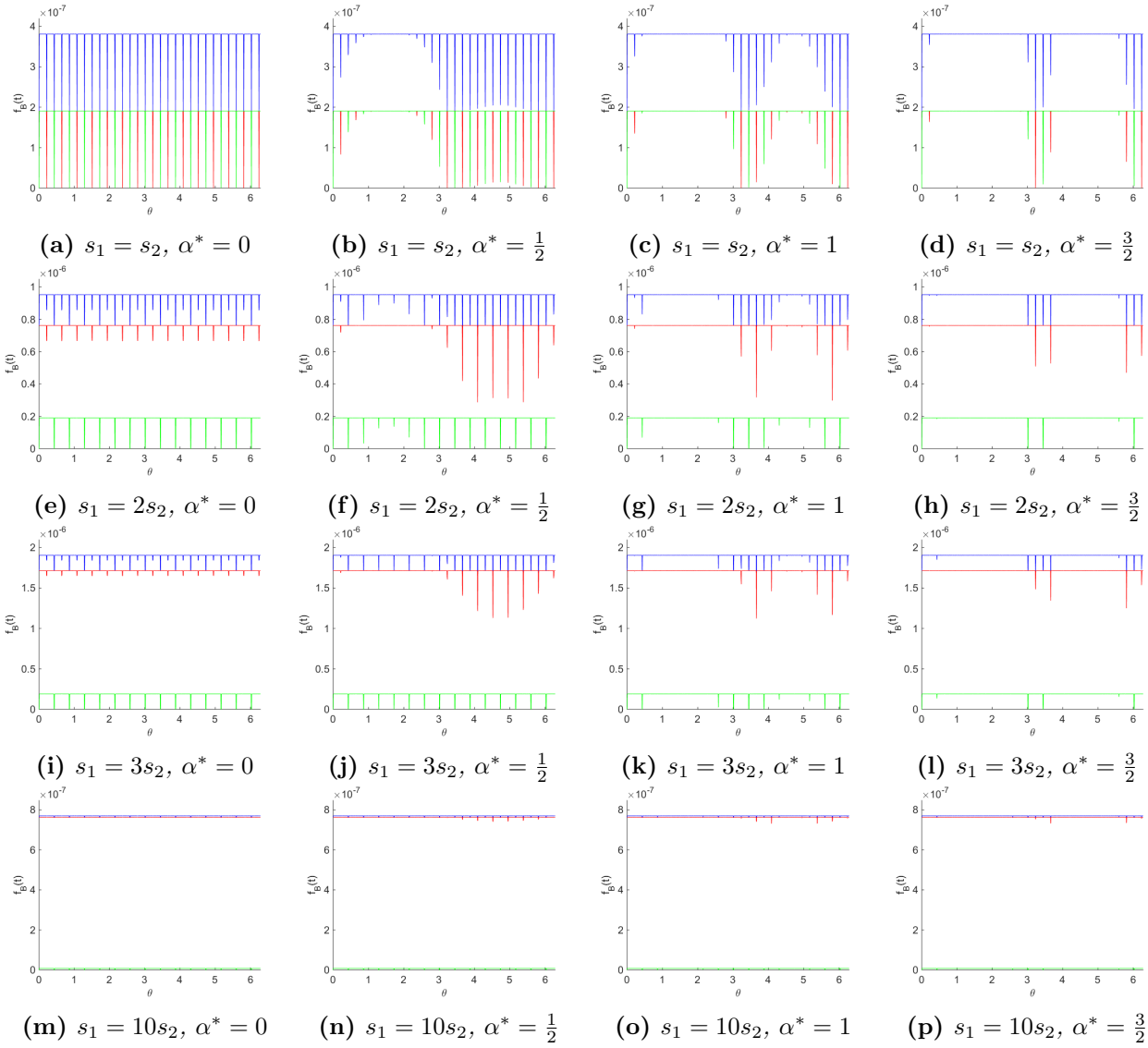

(a) $s_1 = s_2,\ \alpha^* = 0$ **(b)** $s_1 = s_2,\ \alpha^* = \frac{1}{2}$ **(c)** $s_1 = s_2,\ \alpha^* = 1$ **(d)** $s_1 = s_2,\ \alpha^* = \frac{3}{2}$

(e) $s_1 = 2s_2,\ \alpha^* = 0$ **(f)** $s_1 = 2s_2,\ \alpha^* = \frac{1}{2}$ **(g)** $s_1 = 2s_2,\ \alpha^* = 1$ **(h)** $s_1 = 2s_2,\ \alpha^* = \frac{3}{2}$

(i) $s_1 = 3s_2,\ \alpha^* = 0$ **(j)** $s_1 = 3s_2,\ \alpha^* = \frac{1}{2}$ **(k)** $s_1 = 3s_2,\ \alpha^* = 1$ **(l)** $s_1 = 3s_2,\ \alpha^* = \frac{3}{2}$

(m) $s_1 = 10s_2,\ \alpha^* = 0$ **(n)** $s_1 = 10s_2,\ \alpha^* = \frac{1}{2}$ **(o)** $s_1 = 10s_2,\ \alpha^* = 1$ **(p)** $s_1 = 10s_2,\ \alpha^* = \frac{3}{2}$

Figure 5.8: *Reflected light signals for different inclination values and different radii with the observer in the $\hat{z}$-direction. From left to right, the inclination a^* takes on values 0, $\frac{1}{2}$, 1 and $\frac{3}{2}$. From top to bottom, the $\frac{s_1}{s_2}$ takes on values 1, 2, 3, and 10. The red curve is the reflected light signal over the planet f_1, the green curve over the moon f_2 and the blue curve is the total reflected light signal f_B of the bodies.*

When α^* becomes larger, we see that dips (so eclipses) only occur around $\theta = k\pi\ \forall k \in \mathbb{Z}$. This corresponds to the earlier results.

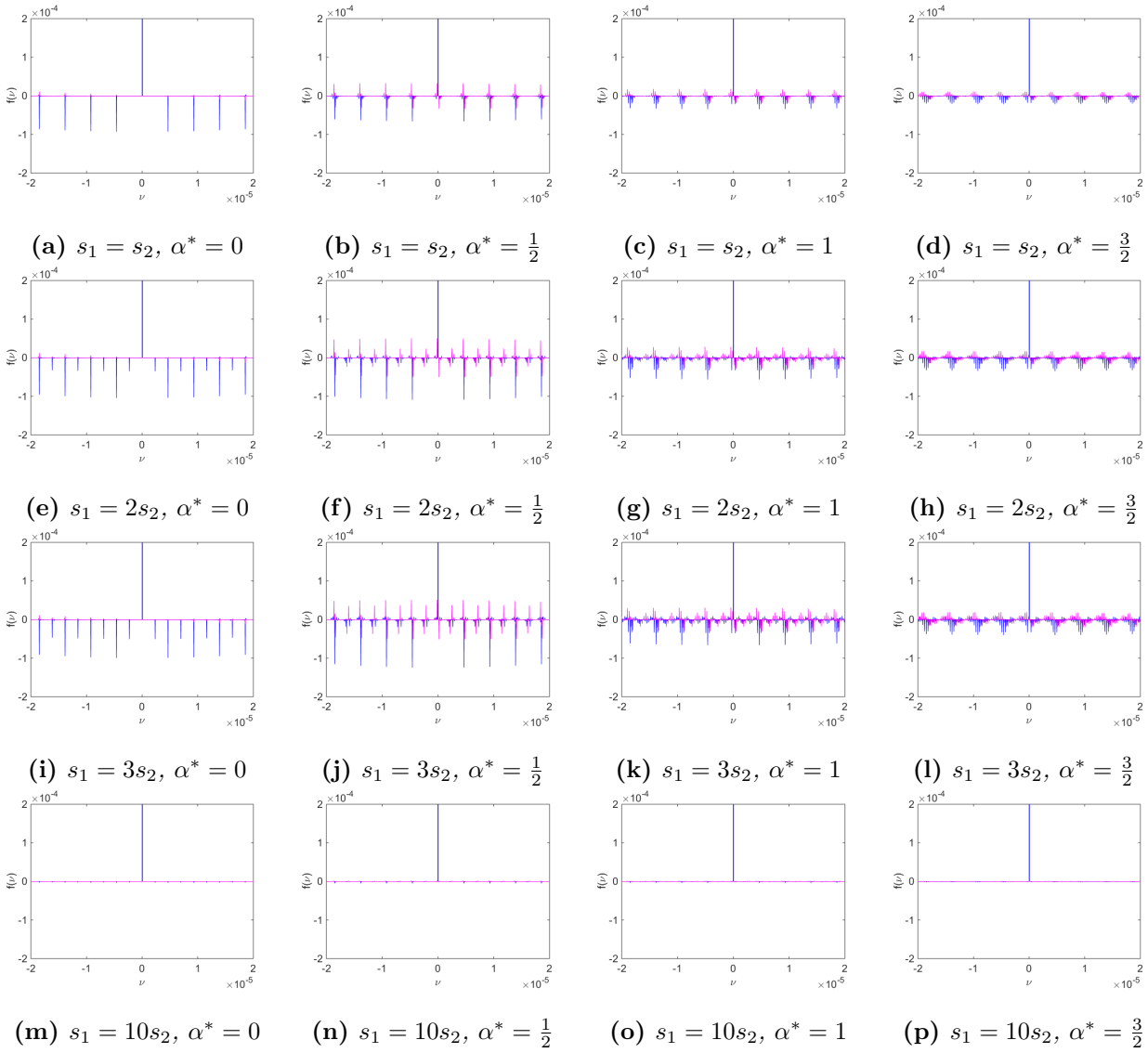

(a) $s_1 = s_2$, $\alpha^* = 0$ **(b)** $s_1 = s_2$, $\alpha^* = \frac{1}{2}$ **(c)** $s_1 = s_2$, $\alpha^* = 1$ **(d)** $s_1 = s_2$, $\alpha^* = \frac{3}{2}$

(e) $s_1 = 2s_2$, $\alpha^* = 0$ **(f)** $s_1 = 2s_2$, $\alpha^* = \frac{1}{2}$ **(g)** $s_1 = 2s_2$, $\alpha^* = 1$ **(h)** $s_1 = 2s_2$, $\alpha^* = \frac{3}{2}$

(i) $s_1 = 3s_2$, $\alpha^* = 0$ **(j)** $s_1 = 3s_2$, $\alpha^* = \frac{1}{2}$ **(k)** $s_1 = 3s_2$, $\alpha^* = 1$ **(l)** $s_1 = 3s_2$, $\alpha^* = \frac{3}{2}$

(m) $s_1 = 10s_2$, $\alpha^* = 0$ **(n)** $s_1 = 10s_2$, $\alpha^* = \frac{1}{2}$ **(o)** $s_1 = 10s_2$, $\alpha^* = 1$ **(p)** $s_1 = 10s_2$, $\alpha^* = \frac{3}{2}$

Figure 5.9: *The Fourier spectra of the reflected light signals seen in figure 5.8 in the $\hat{z}$-direction. From left to right, the inclination a^* takes on values 0, $\frac{1}{2}$, 1 and $\frac{3}{2}$. From top to bottom, the $\frac{s_1}{s_2}$ takes on values 1, 2, 3, and 10. The blue curve is the Fourier transform of the sum of the planets. In every plot, the axes are the same.*

The real and imaginary part of the Fourier spectra of the reflected light signal observed in the $\hat{z}$-direction are plotted in figure 5.9. Again, the side bands indicating eclipses are visible and become spread out when inclination plays a part. The phase curves of the Fourier spectra of the reflected light signal for an observer in the $\hat{z}$-direction is plotted in figure 5.10.

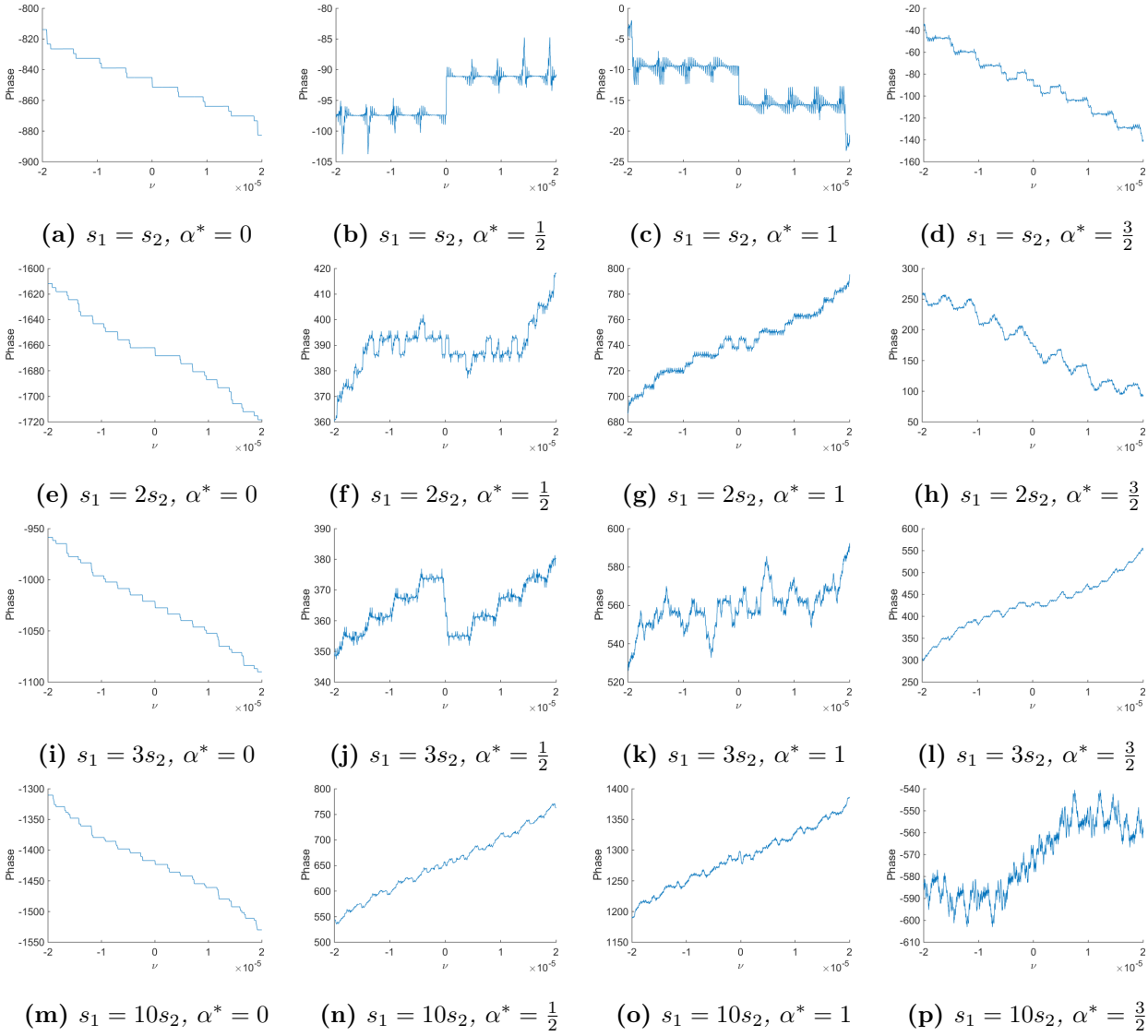

(a) $s_1 = s_2,\ \alpha^* = 0$ **(b)** $s_1 = s_2,\ \alpha^* = \frac{1}{2}$ **(c)** $s_1 = s_2,\ \alpha^* = 1$ **(d)** $s_1 = s_2,\ \alpha^* = \frac{3}{2}$

(e) $s_1 = 2s_2,\ \alpha^* = 0$ **(f)** $s_1 = 2s_2,\ \alpha^* = \frac{1}{2}$ **(g)** $s_1 = 2s_2,\ \alpha^* = 1$ **(h)** $s_1 = 2s_2,\ \alpha^* = \frac{3}{2}$

(i) $s_1 = 3s_2,\ \alpha^* = 0$ **(j)** $s_1 = 3s_2,\ \alpha^* = \frac{1}{2}$ **(k)** $s_1 = 3s_2,\ \alpha^* = 1$ **(l)** $s_1 = 3s_2,\ \alpha^* = \frac{3}{2}$

(m) $s_1 = 10s_2,\ \alpha^* = 0$ **(n)** $s_1 = 10s_2,\ \alpha^* = \frac{1}{2}$ **(o)** $s_1 = 10s_2,\ \alpha^* = 1$ **(p)** $s_1 = 10s_2,\ \alpha^* = \frac{3}{2}$

Figure 5.10: *The phase of Fourier spectra of the reflected light signals in the $\hat{z}$-direction. From left to right, the inclination a^* takes on values 0, $\frac{1}{2}$, 1 and $\frac{3}{2}$. From top to bottom, the $\frac{s_1}{s_2}$ takes on values 1, 2, 3, and 10. The amplitude was shown in figure 5.9.*

6 Conclusion and discussion

The aim of this thesis was to develop a method to detect exomoons or find typical features in the reflection signal that point to the existence of exomoons. To achieve this the reflected light signals of an extra-solar system consisting of one exoplanet (in section 2.4) and an extra-solar system consisting of one exoplanet and one exomoon (in section 3.7) are modeled. The assumptions made are that the bodies have a homogeneous surface (albedo is 1), that the bodies move in a circular motion, and have Lambertian, and that the light from the star is a constant.
We have seen that the important difference between the two systems are eclipses. In section 2.4, we have seen that the reflected light signal of an extra-solar system with one exoplanet is a smooth and continuous periodic graph, due to the periodically changing phases. The maxima were at the phase 'full moon', and the minima at the phase 'new moon'.
In section 3.7 we have seen that the reflected light signal of an extra-solar system with an exoplanet and an exomoon has the same shape as a system with one planet, but is a quasiperiodic signal with dips of short durations. These short dips are the effect of short during eclipses. We deduced that an astronomer could not determine from the signal if an exomoon is present. The astronomer would only know that there is a planet with a periodic disturbance.
In chapter 4 the Fourier spectra of the reflected light signals are calculated. We have found that the Fourier spectrum of the reflected light signal for a system with one planet consists of a series of equidistant δ-peaks. We have seen that the Fourier spectrum has a few peaks at very low frequencies. The other peaks are all nearly zero.
In section 4.3 we split the reflected light signal in two parts, a part due to the phases of the year and a part due to the eclipses. From the Fourier transform of the signal due to the eclipses we deduced that there are peaks that are repeated, so are identical copies. In section 4.2 we have seen those repeated peaks in the figures of the Fourier spectra of the reflected light signal. The repeated peaks indicate short dips in the time-domain.
In chapter 5, an inclination angle was assumed, the ratio of the radii of the bodies was changed and the observer's direction was changed. We have seen that a slight inclination results in shorter during eclipses with less effect. A large inclination angle will cause eclipses at most two times a year. Namely when the exoplanet and exomoon are positioned along the line of intersection between the orbital planes.
An equal sized exoplanet/exomoon ratio and no inclination causes that a planet can be fully darkened by any eclipse. We have seen that a large ratio of the radii causes the eclipse peaks to become small and not really visible with respect to the phase curve.

We conclude that if eclipses occur, the short-during dips in the time-domain give copies in the Fourier domain. So these short dips are characteristics for an eclipse on an exoplanet or exomoon. An astronomer could not tell if the observed signal would result in an exomoon. Other explanations like surface patterns could be the cause of the dips. We cannot yet say if the found light signals would be specific for the presence of an exomoon.
This could be a new method to find binaries and exomoons, but further research is necessary. For instance, we are curious what happens when the surface of the exoplanet and exomoon have an albedo map. For astronomers, it is recommended to find out what the effect of noise is to the signal. The reflected light signal is very small signal. Noise from the star is very common. The signal could become very blurred or not visible at all anymore.

Appendices

A Matlab code for one planet

All data about Jupiter is taken from [25]. Other data is taken from [26] (mass of the Sun), [27] (radius of the Sun) and [28] (Gravitational constant).

```
% Model BEP One planet
% Maaike Mol, 4395913, Applied Mathematics and Applied Physics
%clear all; close all; clc;

% Variables
year = 73;                              % Days per orbit of the barycenter
N = 40*year;                            % Number of timesteps
Orbits = 5;                             % Amount of orbits around star

% Physical quantities
Solar_Mass = 1.99*10^30;                % Solar Mass [kg]
Jupiter_Mass = 1.898*10^27;             % Jupiter Mass [kg]
Radius_Sun = 695700000;                 % Radius Sun [m]
Radius_Jupiter = 69911000;              % Radius Jupiter [m]
omega = 2*pi/(year*24*3600);            % Orbital frequency [rad/s]
rho = Jupiter_Mass/...
    (4/3*pi*(Radius_Jupiter)^3);        % Density of planet [kg m^-3]
s = Radius_Jupiter;                     % Radius planet [m]
S = Radius_Sun;                         % Radius star [m]
G = 6.674*10^(-11);                     % Gravitational con. [m^3 s^-2 kg^-1]
Vol = 4/3*pi*s^3;                       % Volume of planet [m^3]
m = rho*Vol;                            % Mass of planet [kg]
M = 3*Solar_Mass;                       % Mass of star [kg]
R_dist = (G*M/omega^2)^(1/3);           % Distance between star and planet

% Number of measuring steps
Total_Time = Orbits*(year*24*3600); % Time planet orbits around star [s]
dt = Total_Time/N;                      % Time step [s]
N2 = 150;                               % Number of steps in mu
dmu = 2*pi/N2;                          % Step in mu
N3 = 150;                               % Number of steps in nu
dnu = pi/N3;                            % Step in nu
t = 0:dt:Total_Time;                    % Time vector
mu = 0:dmu:(2*pi);                      % Mu vector
nu = 0:dnu:pi;                          % Nu vector

% R vector
R = zeros(3,N+1);
R(1,:) = R_dist*cos(omega*t);
R(2,:) = R_dist*sin(omega*t);
R(3,:) = 0;

% Other vectors
R_normal = zeros(3,N+1);
R_normal(1,:) = cos(omega*t); R_normal(2,:) = sin(omega*t);
R_normal(3,:) = 0;
o_normal = zeros(3,1); o_normal(1,1) = ones(1,1);
```

```
s_normal = zeros(N2+1,N3+1,3);
R_normal_dot = zeros(N2+1,N3+1,3);
o_normal_extended = zeros(N2+1,N3+1,3);
o_normal_extended(:,:,1) = ones(N2+1,N3+1);
s_normal(:,:,1) = cos(mu)'*sin(nu);
s_normal(:,:,2) = sin(mu)'*sin(nu);
s_normal(:,:,3) = ones(N2+1,1)*cos(nu);
s_normal(N2+1,:,:) = 0;

second = dot(s_normal,o_normal_extended,3);

%% Reflected light signal
result = zeros(1,N+1);
for i=1:length(t)
    som = 0;
    R_normal_dot(:,:,1) = ones(N2+1,N3+1)*R_normal(1,i);
    R_normal_dot(:,:,2) = ones(N2+1,N3+1)*R_normal(2,i);
    R_normal_dot(:,:,3) = ones(N2+1,N3+1)*R_normal(3,i);
    first = -dot(R_normal_dot,s_normal,3);
    som = sum((first>0).*(second>0).*first.*second*(sin(nu)'))*(2*pi/N2)
        *(pi/N3);
    result(i) = som;
end
result = result.*s^2./(pi*R_dist^2);

%% Plot
figure()
plot(omega*t,result);
axis([omega*t(1) omega*t(end)+dt/10*omega 0 max(result)+max(result)*0.1])
    ;
ax = gca;
xpoints = 0:(pi):Orbits*2*pi;
ax.XTick = xpoints;
xlabels = {'0','\pi'};
for i=2:length(xpoints)
    xlabels = horzcat(xlabels,strcat(num2str(i),'\pi'));
end
ax.XTickLabel = xlabels;
xlabel('\omega t'); ylabel('f(t)');

%% Fourier
fourier = fft(result,N+1);
Fs = (N+1)/Total_Time;

%Plot in middle
figure;
freqHz = (-(N/2):(N/2))*Fs/(N+1);
fourier = [fourier((N/2+1):(N+1)) fourier(1:(N/2))];
plot(freqHz,real(fourier),'b')
xlabel('\nu [Hz]'); ylabel('f(\nu)')
axis([-3*10^(-5) 3*10^(-5) min(real(fourier)) max(real(fourier))])
set(gca,'fontsize',15);
```

B Matlab code for two planets

```
% Model BEP two planets
% Maaike Mol, 4395913, Applied Mathematics and Applied Physics
clear all; close all; clc;

% Physical quantities
G = 6.674*10^(-11);                 % Gravitational con. [m^3 s^-2 kg^-1]
Solar_Mass = 1.99*10^30;            % Solar Mass [kg]
Mass_J = 1.898*10^27;               % Jupiter Mass [kg]
Radius_J = 69911000;                % Radius Jupiter [m]
Radius_Sun = 695700000;             % Radius Sun [m]
AU = 149597870700;                  % Distance Earth to Sun [m]

% Variables
year = 73;                          % Days per orbit of planet 1 around 2
month = 5;                          % Days per orbit of barycenter
N = 40*month*year;                  % Number of time steps
Orbits = 5;                         % Number of orbits of the barycenter
rho = Mass_J/(4/3*pi*(Radius_J)^3); % Density of the bodies
inclination = 0.5;                    % Inclination value

% Movement quantities
S = 10^9;                           % Radius star [m]
s1 = 2*Radius_J;                    % Radius p1 [m]
s2 = 1*Radius_J;                    % Radius p2 [m]
Vol1 = 4/3*pi*s1^3;                 % Volume of p1
Vol2 = 4/3*pi*s2^3;                 % Volume of p2
M = 3*Solar_Mass;                   % Mass star [kg]
m1 = rho*Vol1;                      % Mass p1 [kg]
m2 = rho*Vol2;                      % Mass p2 [kg]
omega = 2*pi/(year*24*3600);        % Frequency [rad/s]
OMEGA = 2*pi/(month*24*3600)+omega; % Frequency [rad/s]
R_dist = (G*M/omega^2)^(1/3);       % Distance to center of mass [m]
r_dist = (G*(m1+m2)/OMEGA^2)^(1/3); % Distance between two bodies [m]
alpha = inclination*(s1+s2)/r_dist; % Inclination angle [rad]

afstandtotmassamiddelpunt = R_dist/AU;
afstandplaneten = r_dist/AU;

% Calculation duration Eclipse
dt_eclipse = (s1+s2)/((OMEGA-omega)*r_dist);
d_omega_dt_eclipse = omega*dt_eclipse;

% Number of Measuring steps
Total_Time = Orbits*(year*24*3600); % Time planet orbits around the star
    [s]
dt = Total_Time/N;                  % Time step [sec]
N2 = 100;                           % Number of steps in mu
N3 = 100;                           % Number of steps in nu
dmu = 2*pi/N2;
dnu = pi/N3;

```

```
% Code
t = 0:(dt):(Total_Time);
mu = 0:(dmu):(2*pi);
nu = 0:(dnu):pi;

% Rotation matrix
A = [1 0 0; 0 cos(alpha) -sin(alpha); 0 sin(alpha) cos(alpha)];

% Vectors
R = zeros(3,N+1);
R(1,:) = R_dist*cos(omega*t);
R(2,:) = R_dist*sin(omega*t);
R(3,:) = 0;

r = zeros(3,N+1);
r(1,:) = r_dist*cos(OMEGA*t);
r(2,:) = r_dist*sin(OMEGA*t);
r(3,:) = 0;
r = A*r;

R2 = zeros(3,N+1);
R2(1,:) = R(1,:)+m1/(m1+m2)*r(1,:);
R2(2,:) = R(2,:)+m1/(m1+m2)*r(2,:);
R2(3,:) = R(3,:)+m1/(m1+m2)*r(3,:);
R1 = zeros(3,N+1);
R1 = R2-r;

R_normal = zeros(3,N+1);
R_normal(1,:) = cos(omega*t); R_normal(2,:) = sin(omega*t);
R_normal(3,:) = 0;

o_normal_extended = zeros(N2+1,N3+1,3); o_normal_extended(:,:,1) = ones(
    N2+1,N3+1);
s_normal = zeros(N2+1,N3+1,3);

s_normal(:,:,1) = cos(mu)'*sin(nu);
s_normal(:,:,2) = sin(mu)'*sin(nu);
s_normal(:,:,3) = ones(N2+1,1)*cos(nu);
s_normal(N2+1,:,:) = 0;

second = dot(s_normal,o_normal_extended,3);

for i=1:(N+1)
    normR(1,i) = norm(R(:,i));
end
rmatrix = zeros(N2+1,N3+1,3);

% Reflected light signal planet 1 and 2
result1 = zeros(1,N+1);
result2 = zeros(1,N+1);

for i=1:length(t)
    sum1 = 0;
```

```
103     sum2 = 0;
104     lengthR = normR(i);
105
106     R_normal_dot(:,:,1) = ones(N2+1,N3+1)*R(1,i)/lengthR;
107     R_normal_dot(:,:,2) = ones(N2+1,N3+1)*R(2,i)/lengthR;
108     R_normal_dot(:,:,3) = ones(N2+1,N3+1)*R(3,i)/lengthR;
109
110     first1 = -dot(R_normal_dot,s_normal,3);
111     first2 = -dot(R_normal_dot,s_normal,3);
112
113     rmatrix(:,:,1) = ones(N2+1,N3+1)*r(1,i);
114     rmatrix(:,:,2) = ones(N2+1,N3+1)*r(2,i);
115     rmatrix(:,:,3) = ones(N2+1,N3+1)*r(3,i);
116
117     point1 = zeros(N2+1,N3+1,3);
118     point1 = -rmatrix+s1.*s_normal;
119     point2 = zeros(N2+1,N3+1,3);
120     point2 = rmatrix+s2.*s_normal;
121
122     length_for_eclipse1 = cross(point1,R_normal_dot,3);
123     norm3 = sqrt(length_for_eclipse1(:,:,1).^2+length_for_eclipse1(:,:,2)
          .^2+length_for_eclipse1(:,:,3).^2); %N2+1 x N3+1
124     length_for_eclipse2 = cross(point2,R_normal_dot,3);
125     norm4 = sqrt(length_for_eclipse2(:,:,1).^2+length_for_eclipse2(:,:,2)
          .^2+length_for_eclipse2(:,:,3).^2);
126
127     sum1 = sum((first1>0).*(second>0).*not((norm3<s2).*(dot(R(:,i),r(:,i)
          )<0))...
128           .*first1.*second*(sin(nu)')).*(2*pi./N2).*(pi./N3);
129     sum2 = sum((first2>0).*(second>0).*not((norm4<s1).*(dot(R(:,i),r(:,i)
          )>0))...
130           .*first2.*second*(sin(nu)')).*(2*pi./N2).*(pi./N3);
131
132     result1(i) = sum1;
133     result2(i) = sum2;
134 end
135
136 result1 = result1.*s1^2./(pi*R_dist^2);
137 result2 = result2.*s2^2./(pi*R_dist^2);
138
139 %% Plot time domain
140 Result = result1 + result2;
141 figure()
142 hold on;
143 plot(omega*t,Result,'b',omega*t,result1,'r',omega*t,result2,'g')
144 axis([omega*t(1) omega*t(round(1*N/5)) 0 max(Result)+max(Result)*0.1]);
145 %axis([omega*t(1) omega*t(N/5)+dt/10*omega 0 max(Result)+max(Result)
      *0.1]);
146 xlabel('\theta'); ylabel('f_B(t)');
147 set(gca,'fontsize',15);
148
149 % Plot Fourier domain
150 Result = result1 + result2;
```

```
151 Fourier = fft(Result,N+1);
152 Fs = (N+1)/Total_Time; %or 1/dt
153 freqHz = (-(N/2):(N/2))*Fs/(N+1);
154 Fourier = [Fourier((N/2+1):(N+1)) Fourier(1:(N/2))];
155 figure()
156 plot(freqHz,Fourier,'b')%,freqHz,imag(Fourier),'m')
157 xlabel('\nu [Hz]'); ylabel('f(\nu)')
158 % Axis zoom
159 set(gca,'fontsize',15);
160 axis([-3*10^-5 3*10^-5 -4*10^-4 6.5*10^-4])
161
162
163 %% Plot phase of Fourier domain
164 figure()
165 hold on;
166 plot(freqHz,unwrap(angle(Fourier)))
167 xlim([-2*10^-5 2*10^-5]);
168 set(gca,'fontsize',15);
169 xlabel('\nu'); ylabel('Phase');
```

References

[1] Pat Brennan. Exoplanet exploration, 2018. [Online; accessed June 23, 2018].

[2] D. M. Kipping, G. . Bakos, L. Buchhave, D. Nesvorn, and A. Schmitt. The hunt for exomoons with kepler (hek). i. description of a new observational project. *The Astrophysical Journal*, 750(2):115, 2012.

[3] Michelle L. Hill, Stephen R. Kane, Eduardo Seperuelo Duarte, Ravi K. Kopparapu, Dawn M. Gelino, and Robert A. Wittenmyer. Exploring kepler giant planets in the habitable zone. *The Astrophysical Journal*, 860(1):67, 2018.

[4] Dimitri Veras and Elm Breedt. Eclipse, transit and occultation geometry of planetary systems at exo-syzygy. *Monthly Notices of the Royal Astronomical Society*, 468(3):2672–2683, 2017.

[5] The Planetary Society. Transit photometry, 2018. [Online; accessed June 27, 2018].

[6] J. Cabrera and J. Schneider. Detecting Exomoons. In C. Afonso, D. Weldrake, and T. Henning, editors, *Transiting Extrapolar Planets Workshop*, volume 366 of *Astronomical Society of the Pacific Conference Series*, page 242, July 2007.

[7] David M. Kipping. Transit timing effects due to an exomoon. *Monthly Notices of the Royal Astronomical Society*, 392(1):181–189, 2009.

[8] A. E. Simon, Gy. M. Szab, K. Szatmry, and L. L. Kiss. Methods for exomoon characterization: combining transit photometry and the rossitermclaughlin effect. *Monthly Notices of the Royal Astronomical Society*, 406(3):2038–2046, 2010.

[9] András Pál. Light-curve modelling for mutual transits. *Monthly Notices of the Royal Astronomical Society*, 420(2):1630–1635, 2012.

[10] Luis Ricardo M. Tusnski and Adriana Valio. Transit model of planets with moon and ring systems. *The Astrophysical Journal*, 743(1):97, 2011.

[11] Visser, P. M. and van de Bult, F. J. Fourier spectra from exoplanets with polar caps and ocean glint. *A&A*, 579:A21, 2015.

[12] The free encyclopedia Wikipedia. Moons of pluto, 2018. [Online; accessed August 6, 2018].

[13] Murray, C. D. and Correia, A. C. M. Keplerian orbits and dynamics of exoplanets. *Exoplanets*, 579:15–23, 2010. [edited by Seager].

[14] Sanjeev J. Koppal. Lambertian reflectance. In Katsushi Ikeuchi, editor, *Computer Vision: A Reference Guide*, chapter 253, pages 441–443. Springer US, Boston, MA, 2014.

[15] Mauna Kea Astronomy Outreach Committee . Total solar eclipse aug. 21; hawaii partial eclipse begins at dawn, 2017. [Online; accessed May 28, 2018].

[16] Charles Q. Choi. Binary earth-size planets possible around distant stars, 2014. [Online; accessed June 27, 2018].

[17] The free encyclopedia Wikipedia. Charon (maan), 2018. [Online; accessed August 6, 2018].

[18] The free encyclopedia Wikipedia. Pluto, 2018. [Online; accessed August 6, 2018].

[19] The free encyclopedia Wikipedia. Moon, 2018. [Online; accessed August 6, 2018].

[20] The free encyclopedia Wikipedia. Moon, 2018. [Online; accessed August 6, 2018].

[21] The free encyclopedia Wikipedia. Saturn, 2018. [Online; accessed August 6, 2018].

[22] ESA. Facts about titan, 2018. [Online; accessed August 6, 2018].

[23] The free encyclopedia Wikipedia. Titan (moon), 2018. [Online; accessed August 6, 2018].

[24] Luís Miguel Viterbo. How is a new moon different from a lunar eclipse?, 2016.

[25] Ed Grayzeck Nasa Official. Jupiter fact sheet, 2017. [Online; accessed May 28, 2018].

[26] The free encyclopedia Wikipedia. Solar mass, 2018. [Online; accessed June 13, 2018].

[27] The free encyclopedia Wikipedia. Solar radius, 2018. [Online; accessed May 16, 2018].

[28] The free encyclopedia Wikipedia. Gravitatieconstante, 2018. [Online; accessed February 4, 2018].